AGU ADVANCING EARTH AND SPACE SCIENCE

Space Weather

RESEARCH ARTICLE
10.1029/2021SW002800

Key Points:

- Data from cosmic ray neutron sensor (CRNS) networks have been reprocessed and analyzed in the novel context of Space Weather
- Ground level enhancements from solar cycle 24 present weak signals in the data
- Monte Carlo simulations show such CRNS networks are suitable for dual-purposing as space weather detectors

Correspondence to:
A. D. P. Hands,
a.hands@surrey.ac.uk

Citation:
Hands, A. D. P., Baird, F., Ryden, K. A., Dyer, C. S., Lei, F., Evans, J. G., et al. (2021). Detecting ground level enhancements using soil moisture sensor networks. *Space Weather*, *19*, e2021SW002800. https://doi.org/10.1029/2021SW002800

Received 13 MAY 2021
Accepted 22 JUN 2021

Detecting Ground Level Enhancements Using Soil Moisture Sensor Networks

A. D. P. Hands[1], F. Baird[1], K. A. Ryden[1], C. S. Dyer[1], F. Lei[1], J. G. Evans[2], J. R. Wallbank[2], M. Szczykulska[2], D. Rylett[2], R. Rosolem[3], S. Fowler[3], D. Power[3], and E. M. Henley[4]

[1]Surrey Space Centre, University of Surrey, Guildford, UK, [2]UK Centre for Ecology and Hydrology, Wallingford, UK, [3]University of Bristol, Bristol, UK, [4]Met Office, Exeter, UK

Abstract Ground level enhancements (GLEs) are space weather events that pose a potential hazard to the aviation environment through single event effects in avionics and increased dose to passengers and crew. The existing ground level neutron monitoring network provides continuous and well-characterized measurements of the radiation environment. However, there are only a few dozen active stations worldwide, and there has not been a UK-based station for several decades. Much smaller neutron detectors are increasingly deployed throughout the world with the purpose of using secondary neutrons from cosmic rays to monitor local soil moisture conditions (COSMOS). Space weather signals from GLEs and Forbush decreases have been identified in COSMOS data. Monte Carlo simulations of atmospheric radiation propagation show that a single COSMOS detector is sufficient to detect the signal of a medium-strength (10%–100% increase above background) GLE at high statistical significance, including at fine temporal resolution. Use of fine temporal resolution would also provide a capability to detect Terrestrial Gamma Ray Flashes (via secondary neutrons) which are produced by certain lightning discharges and which can provide a hazard to aircraft, particularly in tropical regions. We also show how the COsmic-ray Soil Moisture Observing System-UK detector network could be used to provide warnings at the International Civil Aviation Organization "Moderate" and "Severe" dose rate thresholds at aviation altitudes, and how multiple-detector hubs situated at strategic UK locations could detect a small GLE at high statistical significance and infer crucial information on the nature of the primary spectrum.

Plain Language Summary Space weather events can lead to significant increases in the intensity of the atmospheric radiation environment, including at ground level. These ground level enhancements (GLEs) have been detected by a global network of neutron monitors for over 70 years. However, these instruments are expensive to construct and maintain. Only a few dozen are currently active, with no station located in the United Kingdom for several decades. As part of an effort to improve the resilience of UK infrastructure to space weather, we have studied the possibility of using alternative detectors to supplement neutron monitor measurements. COSMOS detector networks in the United Kingdom, North America, Australia and elsewhere use variations in ground level neutron flux to infer information on local soil moisture conditions for hydrological applications. We show that these same detectors could be dual-purposed to provide information on GLEs that would complement the global neutron monitor network by providing much finer spatial resolution and, therefore, a highly localized warning system for space weather threats to aviation.

1. Introduction

In 2011 the United Kingdom recognized extreme space weather (ESW) events as an example of a high impact natural hazard with a low probability of occurrence in any given year. It was included for the first time as part of the National Risk Assessment, and subsequently added to the National Risk Register (National Risk Register of Civil Emergencies, 2020). In 2013, the Royal Academy of Engineering produced a report on the impacts of ESW on engineered systems and infrastructure (Cannon et al., 2013). The report identified a key risk to infrastructure from another aspect of space weather—relativistic (highly energetic) particles from the Sun. These particles, which are predominantly protons, arrive at Earth without warning as they travel close to the speed of light. In the atmosphere, these generate a multiplicity of secondary particles such as neutrons, electrons and muons. This radiation can directly affect several aspects of critical infrastructure,

from satellites to ground level electronic systems, by causing so-called single event effects (SEE) in microelectronic components. This can lead to disruption, performance degradation and also complete system failure. In addition, effects in human cells leads to significant levels of effective dose to astronauts, aircrew and passengers.

The intensity of the atmospheric neutron environment could increase by many orders of magnitude during an ESW event (Dyer et al., 2018). This is a major concern in the field of avionics and is the subject of a technical report from the International Electro-technical Commission (IEC, 2017) (*Process management for avionics—Atmospheric radiation effects—Part 6: Extreme Space Weather*, 2017). SEE in avionics are of critical importance, but the dose received in-flight by passengers and crew is also a major concern (Dyer et al., 2007; Meier et al., 2020). Although the neutron flux at ground level would be much lower than at aviation altitudes, the amount of exposed infrastructure is far greater and thus an increased SEE rate may still cause disruption. A solar energetic particle event (SEP) that is of sufficient intensity at high energies to cause a significant increase to the ground level neutron flux is known as a ground level enhancement (GLE). These have been recorded on average approximately once per year since instruments capable of such measurements were developed in the 1940s. GLEs are observed by a worldwide network of ground level neutron monitors (GLNMs) (Mishev & Usoskin, 2020). However, there is currently no neutron monitor based in the United Kingdom. Whilst it may be desirable for United Kingdom to have its own fully operational neutron monitor station, existing UK infrastructure may serve as a reasonable proxy source of space weather data. The UK COsmic-ray Soil Moisture Observing System (COSMOS) network of cosmic ray neutron sensors (CRNSs), which infer soil moisture from observations of low energy neutrons reflected from soil via interactions with cosmic-ray generated neutrons, is operated by the UK Centre for Ecology and Hydrology (UKCEH) (Evans et al., 2016). The primary objective of this work is to study the feasibility of dual-purposing the COSMOS sensor network for the purpose of providing a new national resource to enhance the resilience of UK critical infrastructure to space weather hazards. We have examined historic data from cosmic ray neutron sensors in the United Kingdom and elsewhere and explored the potential for technical capability improvements to the UK COSMOS network. Our assessment of the feasibility of providing a sustainable and cost-effective UK space weather measurement capability, potentially providing real-time alerts via the MET Office Space Weather Operations Centre, is described in this study.

2. COSMOS-UK Network

2.1. Description of COSMOS-UK

The COSMOS-UK network is the first national Soil Moisture Monitoring Network in the United Kingdom and was established in 2013. It is operated by UKCEH as part of their UK-SCAPE (National Capability Programme for Environmental Monitoring) and is funded by the Natural Environment Research Council (NERC). There are 50 stations currently operating in England, Scotland, Wales and Northern Ireland, providing research grade hydro-meteorological data (Figure 1 and see Table 1 for site details). Of most relevance to space weather, is the *in situ* ground level measurement of fast or epithermal neutrons at every site by the use of thermal neutron detector proportional counter tubes surrounded by plastic moderator.

The ground-level neutron count rate (once corrected for pressure, humidity etc.) can be related to the soil water content, as the hydrogen atoms in the water are very effective in scattering epithermal-fast neutrons, leading to lower energy (thermalized) neutrons, which are largely excluded from detection by the high-density polyethylene (HDPE) moderator around the neutron detector gas tube. Hence, the soil moisture content can be inversely related to the corrected neutron count (of epithermal-fast neutrons). The current application of the network is for soil moisture measurement, in conjunction with associated weather data. Full details of the COSMOS-UK network can be found at https://cosmos.ceh.ac.uk/ and in Evans et al. (2016) and Cooper et al. (2021).

Zreda et al. (2012) describes the detector principle and configuration. These are gas-filled detectors and, for the most common sensor type in the COSMOS-UK network, CRS-2000/B (Figure 2), thermal neutrons (generated by moderation of the epithermal-fast neutrons by the HDPE moderator around the detector) are captured by boron-10 in the form of boron trifluoride (BF_3). The charged reaction products of neutron capture by ^{10}B and the resulting ionization are in turn detected by application of a high voltage (~1,000 V)

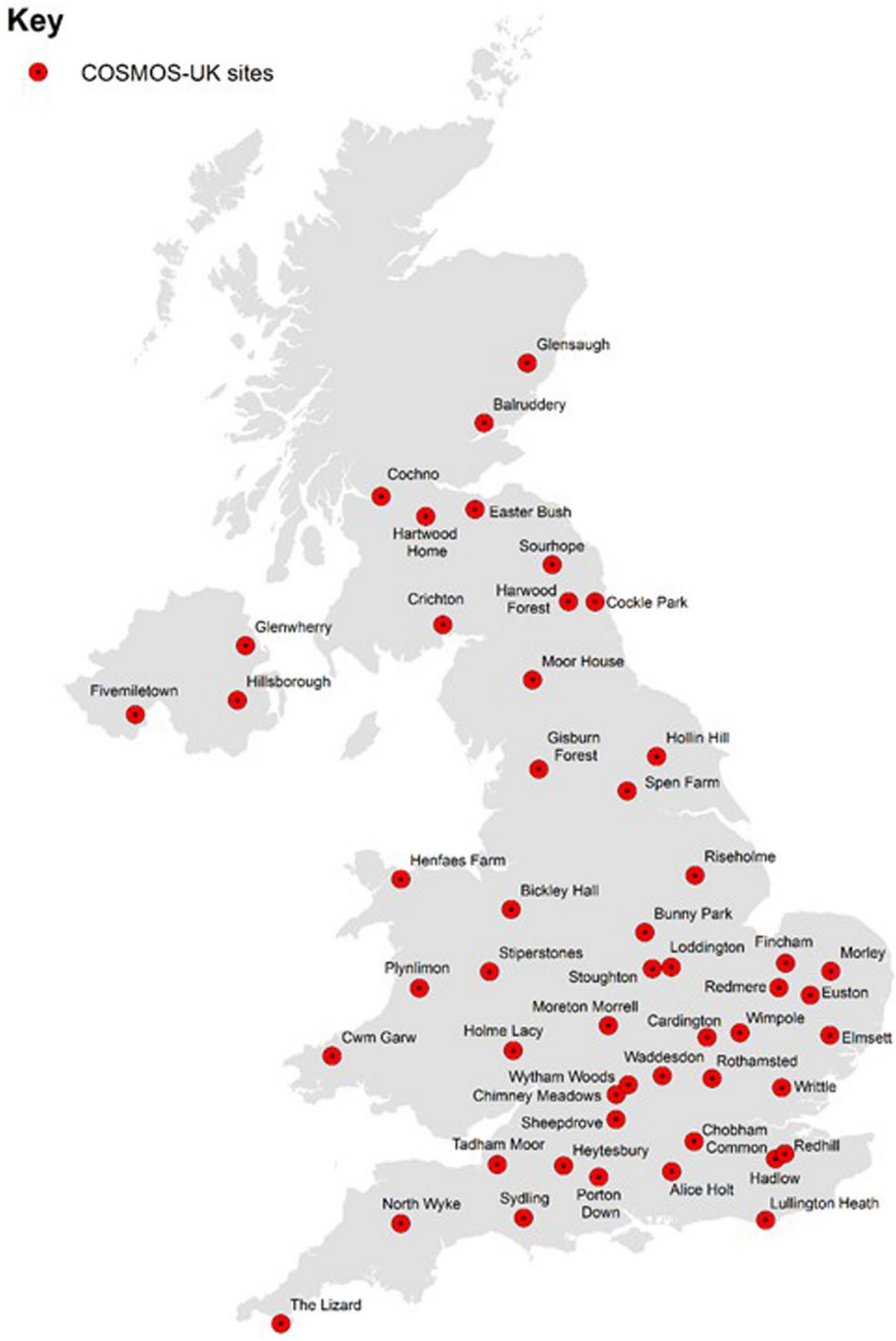

Figure 1. Map of COsmic-ray Soil Moisture Observing System-UK sites.

across the gas tube (the tube wall acts as the cathode, and the anode is a thin wire running down the central axis of the tube). A neutron pulse module, model NPM-2000 (Quaesta Instruments, Arizona, USA), provides digital pulse-height discrimination and cumulative counts of neutrons, as well as a high voltage supply for the gas tube. Data processing typically adjusts for variations in atmospheric pressure, humidity, and the intensity of incoming cosmic rays, however the last of these (which is based on the Jungfraujoch neutron monitor) is not applied in our analysis as we need to retain this signal.

Table 1
List of COSMOS-UK Stations and Location Details

Ref. #	Name	Abbr.	Latitude	Longitude	Altitude (m)	Rigidity (GV)	Date range
19	Glensaugh	GLENS	56.91440	−2.56215	399	1.54	May 2014–November 2019
6	Balruddery	BALRD	56.48230	−3.11149	130	1.60	May 2014–November 2019
50	Cochno	COCHN	55.94142	−4.40354	168	1.66	August 2017–November 2019
22	Hartwood Home	HARTW	55.81026	−3.82896	225	1.70	May 2014–November 2019
15	Easter Bush	EASTB	55.86741	−3.20709	208	1.71	August 2014–November 2019
40	Sourhope	SOURH	55.47988	−2.22999	487	1.80	November 2014–November 2019
20	Glenwherry	GLENW	54.83809	−6.00460	274	1.82	June 2016–November 2019
14	Crichton	CRICH	55.04312	−3.58337	42	1.84	December 2014–November 2019
23	Harwood Forest	HARWD	55.21594	−2.02355	300	1.86	May 2015–November 2019
13	Cockle Park	COCLP	55.21601	−1.69437	87	1.87	November 2014–November 2019
25	Hillsborough	HILLB	54.44700	−6.06840	146	1.91	June 2016–November 2019
1	Fivemiletown	FIVET	54.29850	−7.29186	174	1.92	June 2018–November 2019
30	Moor House	MOORH	54.65942	−2.46780	565	1.96	December 2014–November 2019
18	Gisburn Forest	GISBN	54.02381	−2.38463	246	2.11	August 2014–November 2019
26	Hollin Hill	HOLLN	54.11068	−0.95952	82	2.13	March 2014–November 2019
46	Spen Farm	SPENF	53.86886	−1.31886	57	2.17	November 2016–November 2019
24	Henfaes Farm	HENFS	53.22541	−4.01244	287	2.24	December 2015–November 2019
7	Bickley Hall	BICKL	53.02635	−2.70053	78	2.33	January 2015–November 2019
37	Riseholme	RISEH	53.26165	−0.52591	53	2.33	May 2016–November 2019
8	Bunny Park	BUNNY	52.86073	−1.12685	39	2.41	January 2015–November 2019
42	Stiperstones	STIPS	52.58125	−2.94469	432	2.42	November 2014–November 2019
33	Plynlimon	PLYNL	52.45338	−3.76259	542	2.43	November 2014–November 2019
41	Stoughton	STGHT	52.60164	−1.04701	130	2.47	August 2015–November 2019
28	Loddington	LODTN	52.61016	−0.82642	186	2.47	April 2016–November 2019
47	Fincham	FINCH	52.61777	0.51073	15	2.49	June 2017–November 2019
31	Morley	MORLY	52.54815	1.03423	55	2.51	May 2014–November 2019
10	Cwm Garw	CGARW	51.95136	−4.74658	299	2.52	June 2016–November 2019
35	Redmere	RDMER	52.44577	0.42104	3	2.53	February 2015–September 2018
48	Moreton Morrell	MOREM	52.19941	−1.56308	53	2.54	November 2018–November 2019
17	Euston	EUSTN	52.38318	0.78471	18	2.54	March 2016–November 2019
51	Holme Lacy	HLACY	52.02088	−2.66211	76	2.56	April 2018–November 2019
9	Cardington	CARDT	52.10560	−0.42464	29	2.59	June 2015–November 2019
3	Wimpole	WIMPL	52.13219	−0.04441	30	2.60	September 2019–November 2019
16	Elmsett	ELMST	52.09465	0.99306	76	2.61	August 2016–November 2019
44	Waddesdon	WADDN	51.83948	−0.94842	98	2.64	November 2013–November 2019

Table 1
Continued

Ref. #	Name	Abbr.	Latitude	Longitude	Altitude (m)	Rigidity (GV)	Date range
45	Wytham Woods	WYTH1	51.77728	−1.33846	109	2.64	November 2013–September 2016
11	Chimney Meadows	CHIMN	51.70802	−1.47877	65	2.66	October 2013–November 2019
38	Rothamsted	ROTHD	51.81387	−0.37832	131	2.66	July 2014–November 2019
4	Writtle	WRTTL	51.73400	0.41790	44	2.69	July 2017–November 2019
39	Sheepdrove	SHEEP	51.53032	−1.48187	170	2.70	October 2013–November 2019
43	Tadham Moor	TADHM	51.20750	−2.82879	7	2.74	October 2014–November 2019
12	Chobham Common	CHOBH	51.36795	−0.59748	47	2.75	February 2015–November 2019
2	Heytesbury	HYBRY	51.20289	−2.07960	166	2.76	August 2017–November 2019
34	Porton Down	PORTN	51.11988	−1.68125	146	2.78	December 2014–November 2019
36	Redhill	REDHL	51.26287	0.42913	91	2.79	February 2016–November 2019
5	Alice Holt	ALIC1	51.15355	−0.85823	80	2.79	March 2015–November 2019
21	Hadlow	HADLW	51.22856	0.32018	33	2.80	October 2016–November 2019
32	North Wyke	NWYKE	50.77348	−3.90596	181	2.81	October 2014–November 2019
49	Sydling	SYDLG	50.82837	−2.52789	249	2.83	November 2018–November 2019
29	Lullington Heath	LULLN	50.79372	0.18887	119	2.90	December 2014–November 2019
27	The Lizard	LIZRD	50.03281	−5.19988	85	2.96	October 2014–November 2019

Note. Sites are ordered by increasing rigidity cut-off and date ranges for data used in this analysis are given for each station.
Abbreviation: COSMOS, COsmic-ray Soil Moisture Observing System.

3. Space Weather Sensitivity in Existing COSMOS Data

Space weather can lead to both increases and decreases in the ground level atmospheric radiation environment. Forbush decreases (Lockwood, 1971; Lockwood et al., 1991) are relatively common and have been observed in soil moisture sensors before (Schrön, 2017). Our analysis of these events in recent COSMOS data will be reported in a separate article. GLEs, by contrast, occur at an average rate of one per year (Asvestari et al., 2017; Miroshnichenko, 2018). COSMOS detectors have been deployed in the United Kingdom and North America for approximately one decade. In that timeframe two GLEs were recorded by the GLNM network: GLE #71 on May 17, 2012 (Mishev et al., 2014) and GLE #72 on September 10, 2017 (Jiggens et al., 2019; Mishev & Usoskin, 2018). As can be seen with Oulu neutron monitor data plotted in Figure 3, neither event was large by historical context. GLE71 produced ∼15% increases at Oulu in Finland and Apatity in Russia, and at the high-altitude South Pole station. Increases in Canadian low rigidity cut-off neutron monitors were more modest at ∼5%. GLE72 was even smaller with only the high-altitude Antarctic mini neutron monitors DOM-B and DOM-C registering increases in excess of 10%. For both GLEs only neutron monitors at low rigidity cut-off (<2 GV) observed any significant increase over the GCR background count rate.

This absence of large GLEs in recent years means the scope for discovering GLE signals in COSMOS detector data is extremely limited. This is especially true for the UK COSMOS network because, with the exception of one station, processed data are only available since late 2013. A list of station names, coordinates and cut-off rigidities for the UK COSMOS network is given in Table 1.

COSMOS-UK counts are collected in 30-min bins and raw count rates are then corrected for atmospheric pressure (Zreda et al., 2012) and humidity (Rosolem et al., 2013). Figure 4 shows the full range of data available for the Alice Holt station in Hampshire and Figure 5 shows these data for the period around GLE72 only. In both cases uncorrected counts, corrected counts and 24-h smoothed corrected counts are plotted.

Figure 2. COsmic-ray Soil Moisture Observing System-UK detector at the Easter Bush site (model shown is a CRS-2000/B sensor made by Hydroinnova LLC, New Mexico, USA).

Various quality flags are also applied to the corrected count rates. The two dominant influences on the fluctuation of the count rate after pressure and humidity correction are cosmic ray modulation and variation in local soil moisture conditions. In Figure 5 there is also significant statistical fluctuation over short timescales, of the order of 5%, which is consistent with Poisson uncertainty on ~600 counts per bin. The planetary Kp index at the time of GLE72 was 2, which corresponds to a rigidity cut-off of 2.7 GV for Alice Holt (for comparison, the cut-off rigidity at Kp = 0 is 2.8). This means that we would not expect to see statistically significant evidence of GLE72 in the data, and indeed Figure 5 confirms that this is the case. The same can be said for the higher latitude COSMOS-UK station of Balruddery (Scotland), which at the time of GLE72 had a cut-off rigidity of 1.5 GV. Figure 5 (RHS) shows that there is no statistically significant spike in corrected count rate (black dots) coincident with the peak of GLE72.

Unfortunately, the only UK COSMOS station for which data are available during GLE71 (May 17, 2012) is Sheepdrove (in southern UK, so with a high rigidity cut-off of 2.7 GV). This station utilizes an earlier detector design (CRS1000/B) compared to most of the rest of the network, which results in a significantly lower count rate. Figure 6 shows the Sheepdrove count rate around the time of GLE71, as well as equivalent smoothed count rates for GLNM stations at Oulu and Kiel (rigidity cut-offs 0.8 and 2.7 GV respectively). The comparison shows that, not only would a 10%–15% increase in count rate be difficult to resolve given the statistical fluctuation in the COSMOS count rate, but also crucially that no such increase should be expected at a location with a cut-off rigidity as high as at Sheepdrove. We can, therefore, effectively rule out any possibility of observation of GLE71 in UK COSMOS data.

Fortunately, 43 of the 51 COSMOS-UK stations recorded data around GLE72. To improve the potential for resolving small increases in the count rate, we have aggregated the data for all available stations in the period. Figure 7 shows both individual station data and average count rate. A small peak (<2% increase) is observed to be coincident with GLE72, however, the magnitude is on a par with other nearby peaks and consistent with simple statistical fluctuation, so it is inconclusive whether GLE72 is wholly or partly responsible for this peak.

North American COSMOS stations occupy locations with lower cut-off rigidity than COSMOS-UK stations. Table 2 lists the nine stations with the lowest cut-off rigidity (all under 1.5 GV), which we have used in our GLE analysis. Location and rigidity information was sourced from http://cosmos.hwr.arizona.edu/, where some raw and processed data are also available for download. Data used in the following analysis were separately obtained and reprocessed as part of the MOSAIC project using the newly developed Cosmic-Ray Sensor PYthon tool (crspy—Power et al., 2021). Crspy is a comprehensive open-source data processing tool (https://github.com/danpower101/crspy) which includes all up-to-date knowledge about the technology and can be used for a wide variety of applications (e.g., hydrology and space weather). Three correction factors are applied for atmospheric pressure (Zreda et al., 2012), atmospheric water vapor (Rosolem et al., 2013) and above ground biomass (Baatz et al., 2015). Additionally, for soil moisture readings, site calibration is required that has been improved upon since the first inception of these sensors (Schrön et al., 2017). The temporal resolution of all raw data is 1 h binning of detector counts. Corrected count rates are shown for all available time periods for each station in Figure 8.

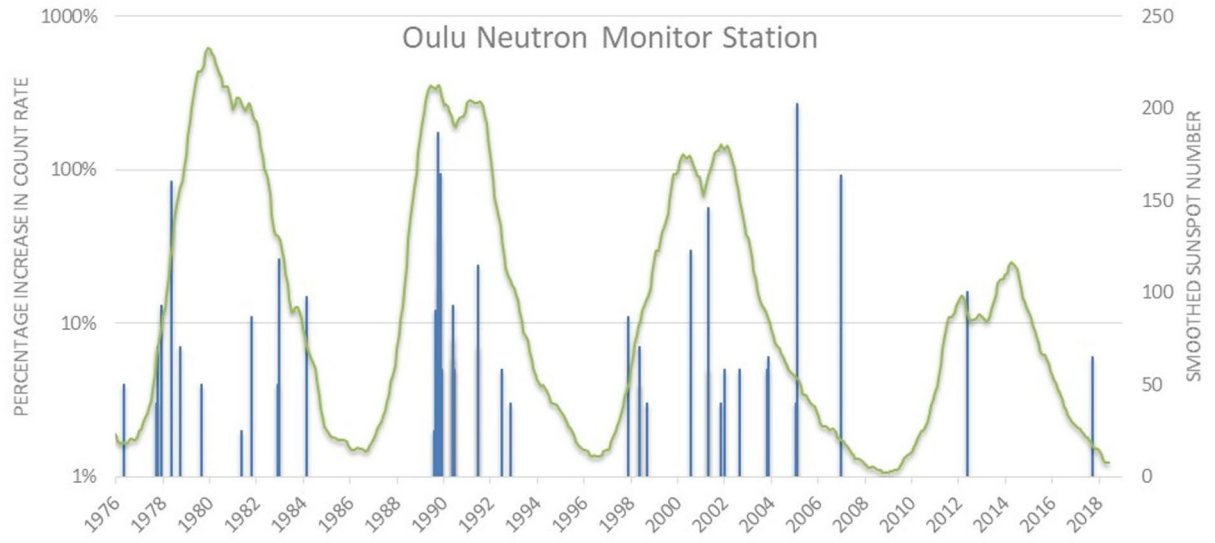

Figure 3. Ground level enhancement percentage increases since 1976 measured at the OULU neutron monitor in Finland (blue bars). A smoothed sunspot number (green line) is also plotted to show the solar cycle context (http://www.sidc.be/silso/).

Seasonal effects in the count rates due to local soil moisture variation and snow accumulation are apparent in the data. As is also clear from Figure 8, not all stations have data available for either or both GLEs. Table 2 summarizes which stations have data for each GLE—three for GLE71 and seven for GLE72. Although the Saskatoon station has no data for either GLE, the data set is included in the analysis as it is useful to compare rates of false positive GLE identification.

Figures 9 and 10 show all reprocessed COSMOS data for the periods around GLE71 and GLE72 respectively. Due to the relatively low count rate at each station, the data have been rebinned into 4-h intervals to improve the counting statistics. In both cases, there is a small spike in the averaged count rate data coincident

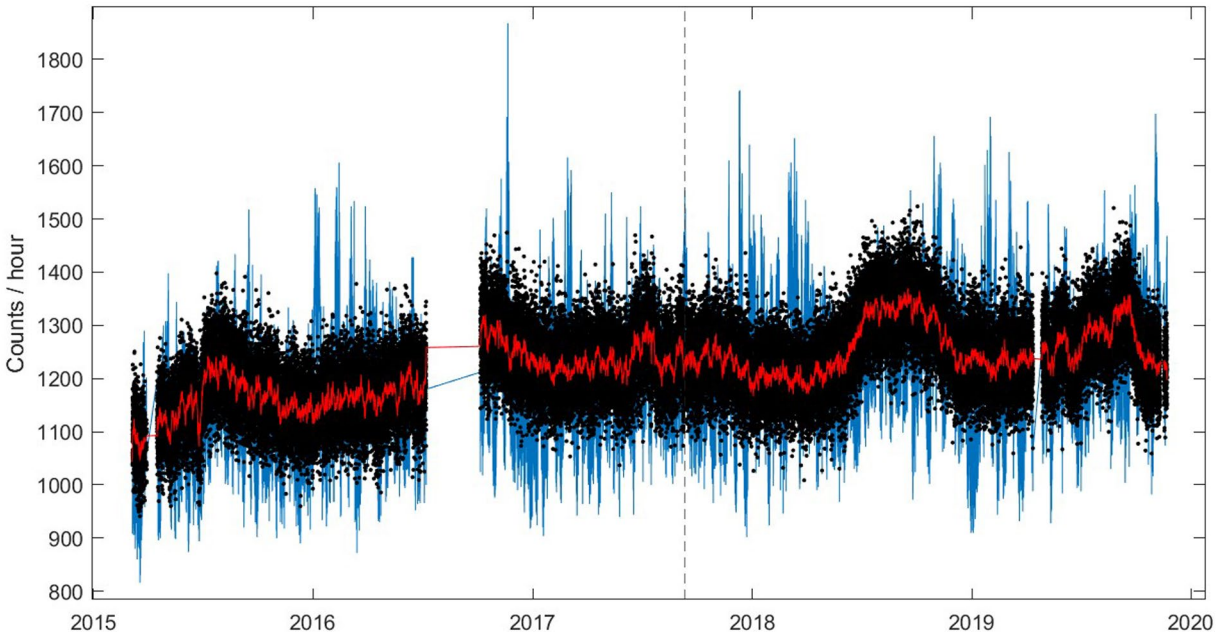

Figure 4. Data from the Alice Holt COsmic-ray Soil Moisture Observing System station. The uncorrected count rate, corrected count rate and 24-h smoothed corrected count rate are represented by the blue line, black dots and red line respectively. Ground level enhancement72 is represented by a dashed vertical black line.

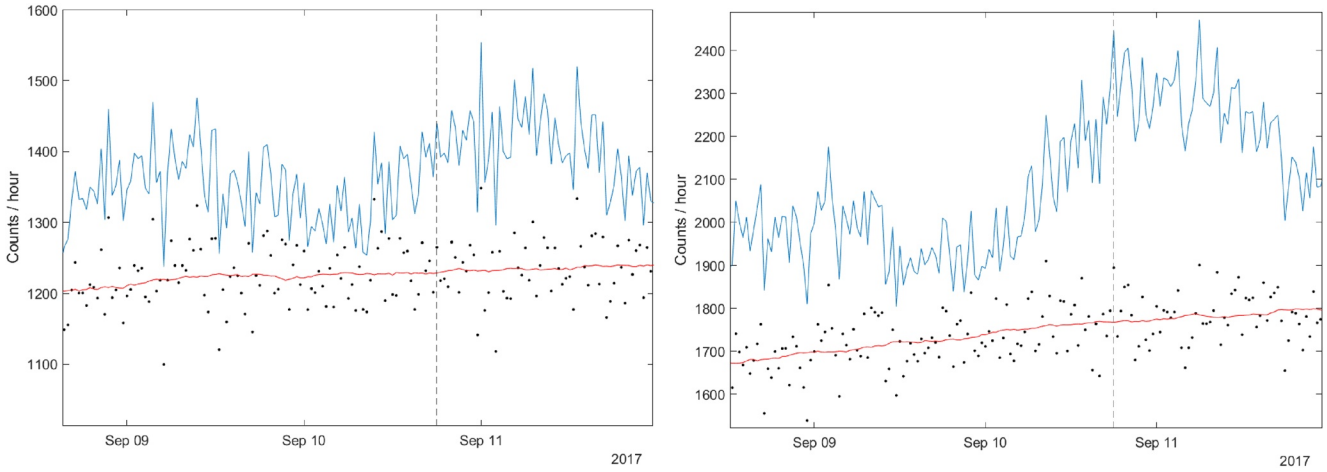

Figure 5. Alice Holt (LHS) and Balruddery (RHS) data for the period of time before and after Ground level enhancement (GLE72). The uncorrected count rate, corrected count rate, and 24-h smoothed corrected count rate are represented by the blue line, black dots and red line respectively. GLE72 is represented by a dashed vertical black line.

with the GLE. However, in the case of GLE71 the spike is indistinguishable from similar spikes nearby, and hence is consistent with statistical fluctuation. In the case of GLE72 the coincident spike appears more significant, though this appearance is helped substantially by the presence of a significant Forbush decrease in the data immediately before the GLE.

To investigate the significance of GLE signals in the individual station data we devised a simple statistical test that can be applied to any of the data series:

$$\text{Significance}\left(\text{S}\right) = \frac{\text{Increase in count rate}\left(\text{compared to previous 24 hrs}\right)}{\text{Average Poisson error of previous 24 hours}} = \frac{\Delta \text{N}}{\bar{\sigma}_{\text{P}}} \quad (1)$$

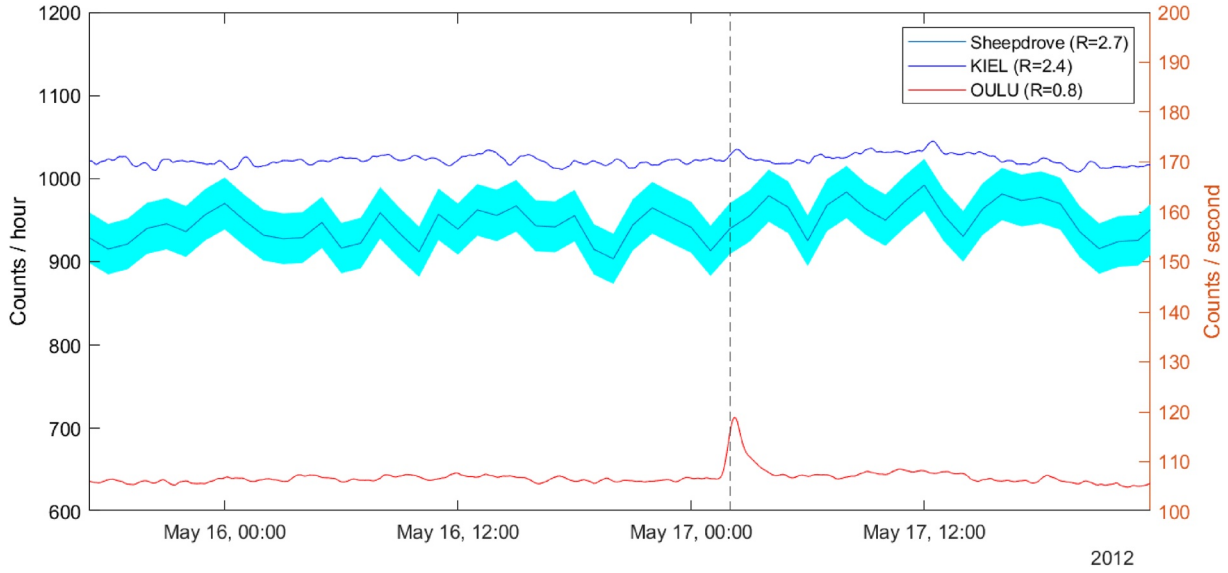

Figure 6. Count rate data from Sheepdrove COsmic-ray Soil Moisture Observing System (COSMOS-UK) station around the time of ground level enhancement71 (indicated with a dashed vertical line). The shaded area around the Sheepdrove count rate represents an uncertainty band due to Poisson statistics. Additional count rates for KIEL and OULU neutron monitors are also plotted (right hand vertical axis), each has been smoothed to hourly resolution for comparison with COSMOS.

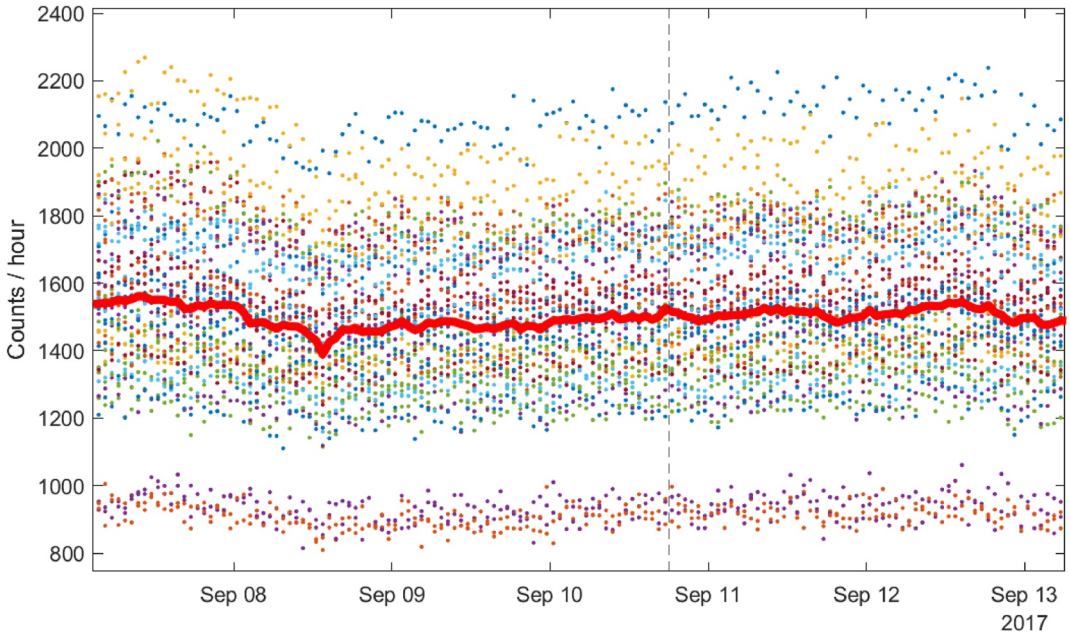

Figure 7. Corrected count rates from 43 UK COsmic-ray Soil Moisture Observing System stations (dots) and average count rate (red line) during the period surrounding ground level enhancement (GLE72). The data have been rebinned into common hourly intervals. The peak of GLE72 is represented by a dashed vertical black line.

We calculate a value for significance (S) for every data point in a 4-h temporal binning scheme. For example, Figure 11 shows the corrected count rate for the Park Falls COSMOS station in May 2012. The count rate coincident with GLE71 is 1,258 counts/hour, compared to an average count rate in the preceding 24 h of 1,220 counts/hour. The average Poisson error of the six bins in the preceding 24-h period is 18.7 counts/hour, hence using Equation 1 the calculated significance parameter is $S = 2$.

To put this value for S in context, we repeated this calculation for the entire data series. Figure 12 shows Park Falls data for the entire available period, with the corresponding value of S. The distribution of S is plotted as a histogram in Figure 13. It is clear from these plots that the value of S at GLE71 ($S = 2$) does not represent an outlier in the Gaussian-like distribution.

We applied this process to all seven of the other low rigidity COSMOS stations with data during one or both GLEs, and to Saskatoon, which has data for neither. The results for stations 43, 48, 88, and 94 are shown in

Table 2
North American COSMOS Stations With the Lowest Cut-Off Rigidity

Site ID	Site name	Latitude	Longitude	Altitude (m)	Rigidity (GV)	GLE71	GLE72
97	Trail Valley Main Met	68.7455	−133.5	125	0.06	x	✓
94	Trail Valley Upper Plateau	68.6936	−133.6974	150	0.09	x	✓
96	Havikpak Main Met	68.3199	−133.5198	125	0.09	x	✓
95	Trail Valley Forest	68.7227	−133.4955	125	0.1	x	✓
105	Barrow-ARM	71.3298	−156.6287	4	0.14	x	✓
88	Saskatoon	52.1326	−106.6168	506	0.86	x	x
48	Fort Peck	48.3077	−105.1019	634	1.23	✓	✓
42	Park Falls	45.9459	−90.2723	470	1.25	✓	x
43	UMBS	45.5598	−84.7138	220	1.31	✓	✓

Note. GLE data coverage for each COSMOS station is also indicated.
Abbreviations: COSMOS, COsmic-ray Soil Moisture Observing System; GLE, ground level enhancement.

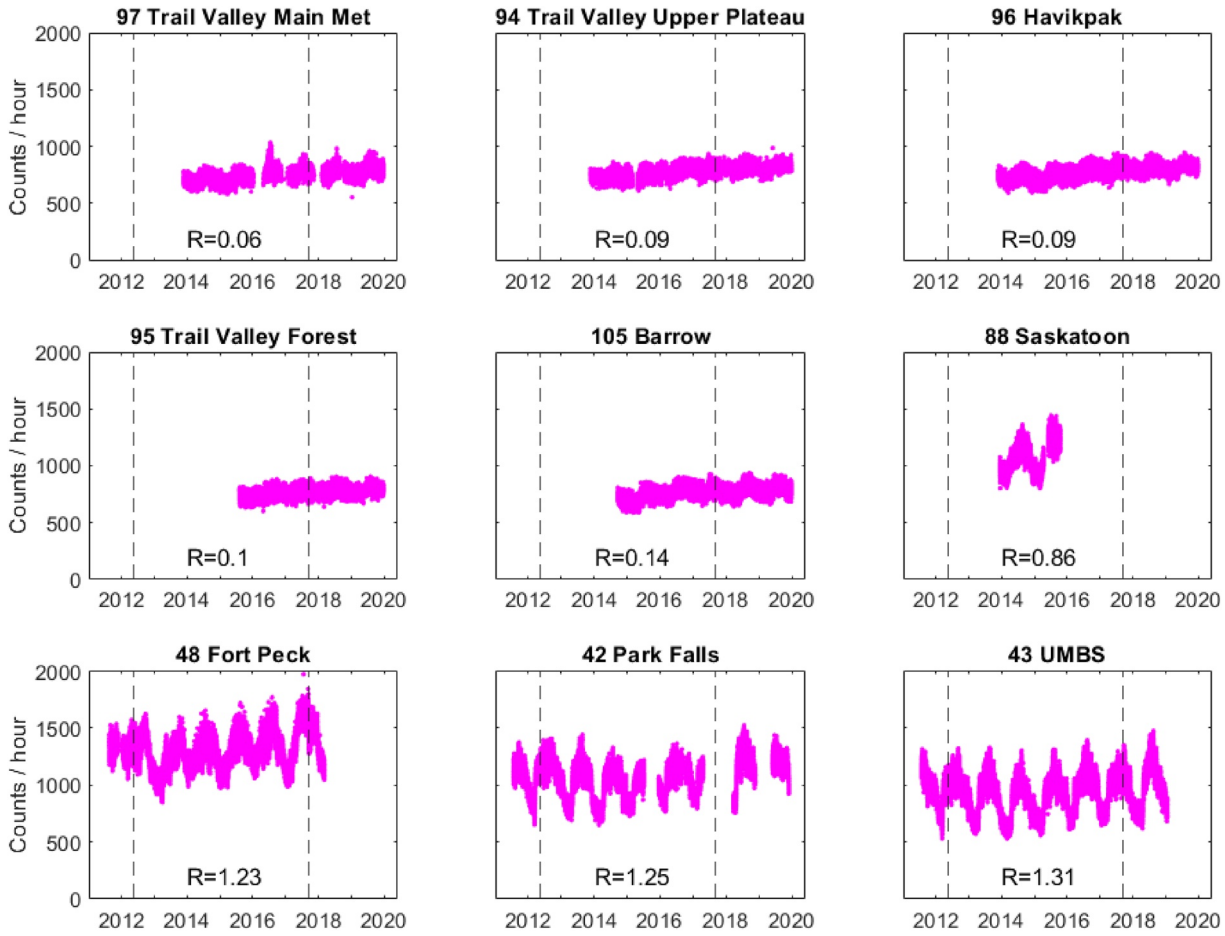

Figure 8. Corrected count rates for nine North American COsmic-ray Soil Moisture Observing System stations. Ground level enhancement (GLE71) and GLE72 are represented by dashed vertical black lines. Rigidity values are embedded in each subfigure.

Figure 14, results for stations 95, 96, 97, and 105 are shown in Figure 15. Gaps in the upper panel (S) time series that are not present in the lower panel (count rate) time series are present because we imposed a condition that, for a value of S to be calculated, the data for the previous 24 h must be complete (see Equation 1). Red lines in the S data series are used to highlight instances where $S > 5$.

On this scale the values of S at the time of each GLE cannot be read directly from the plots. Table 3 summarizes the calculated values for all stations, as well as the number of occasions where an S value greater than 5 was recorded (hereafter referred to as "false positives" in the vast majority of cases where these data points are not coincident with a GLE).

Table 3 shows that there is only one station where either GLE coincided with an S value greater than five. This was for GLE72 in the Barrow data set. Figure 16 shows a zoomed-in version of the binned data series and S values for this period. GLE72 coincides with a clear spike in the COSMOS data, however the significance ($S = 6.9$) is enhanced by the Forbush decrease that occurs immediately beforehand. The prominence of the peak relative to the period *after* the GLE is lower. This introduces doubt into the true significance of the peak in the Barrow data. To further illustrate this, Figure 17 shows renormalized count rates for all seven COSMOS stations with data during GLE72. Plotted on the same relative axis is the count rate for the Inuvik (INVK) neutron monitor station, which is in very close geographical proximity to the three Trail Valley COSMOS stations (#s 94, 95, & 97) and Havikpak (#96), as depicted in Figure 18.

The magnitude of the increase at Inuvik is ~6% relative to the period immediately prior to the event (though this level is depressed due to the ongoing Forbush decrease and is reduced to ~4% if an equivalent 4-h averaging scheme is used). Renormalized count rates for the four COSMOS stations in close proximity to Inuvik

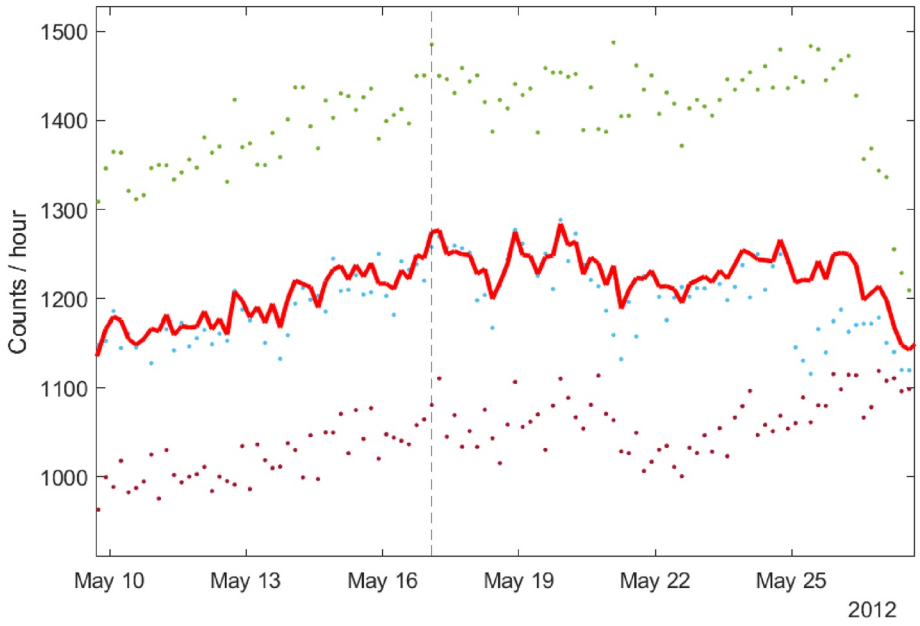

Figure 9. Individual COsmic-ray Soil Moisture Observing System station data (colored dots) and average (red line) for the period surrounding GLE71. All data are binned into 4-h intervals to further improve the statistics. The ground level enhancement is represented by a dashed vertical black line.

show fluctuations that are of the same order of magnitude as the increase at Inuvik but, due to the lower count rate, do not carry the same statistical significance. By contrast the peak at Barrow is approximately twice the size implied by neutron monitor data. Although the distance between Barrow and Inuvik is nearly 1,000 km, this excess is unlikely to be caused by longitudinal anisotropy in the GLE as several other neutron monitors spanning a wide longitudinal range (Thule, Peawanuck and Nain) all show increases in the 4%–6% range.

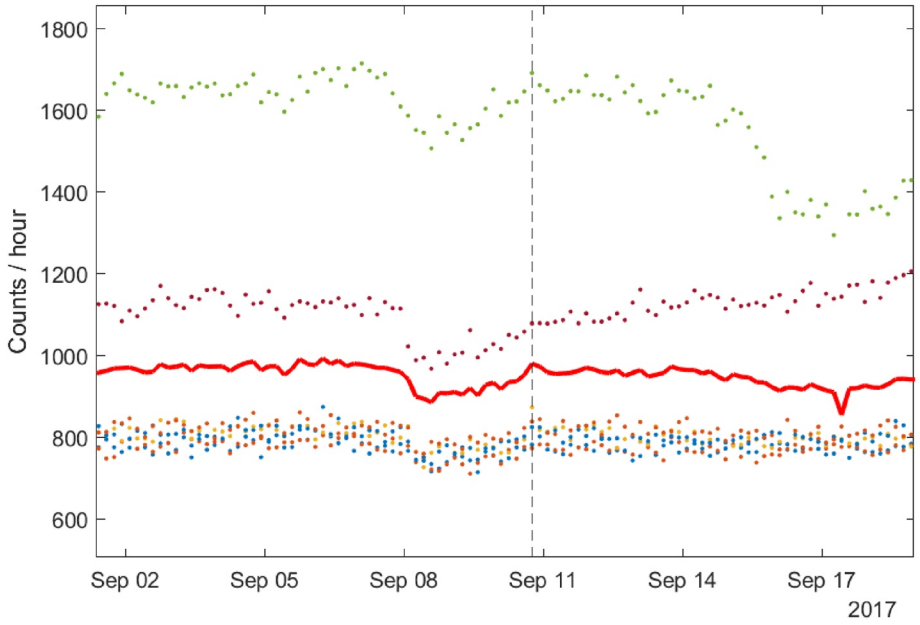

Figure 10. Individual COsmic-ray Soil Moisture Observing System station data (colored dots) and average (red line) for the period surrounding GLE72. All data are binned into 4-h intervals to further improve the statistics. The ground level enhancement is represented by a dashed vertical black line.

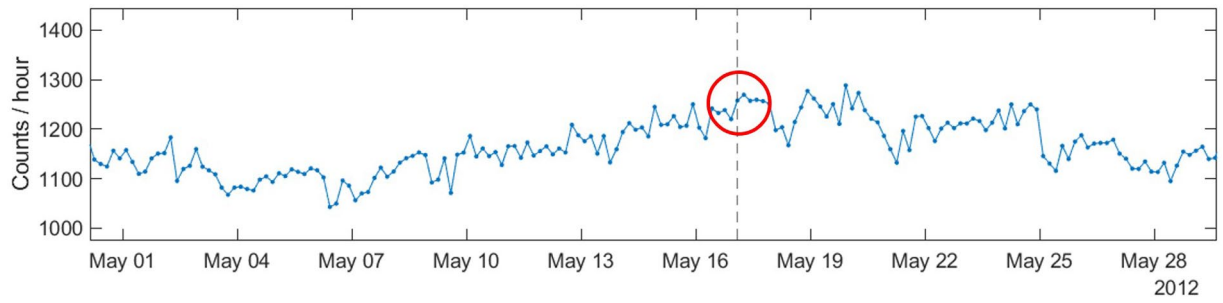

Figure 11. Corrected count rate of Park Falls COsmic-ray Soil Moisture Observing System station in May 2012. The data are binned in 4-h intervals and the data point coincident with GLE71 (counts recorded from 00:00–04:00 on May 17, 2012) is highlighted with a red circle.

Another factor that may play a role in the prominence of the peak at Barrow is the local soil moisture conditions at the time of GLE72. Figure 19 shows again the 4-h binned count rate at Barrow, with ERA5-Land hourly rainfall data plotted below on the same time axis. The rainfall data are based on a remodeled gridded data set with 9 km spatial resolution rather than rainfall gauges co-located with the COSMOS detector. The data from the Barrow region indicate that rainfall did occur in the area prior to the event and coincident with the early stages of the Forbush decrease. Hence it is possible that there is an underlying gradual increase in count rate caused by the drying of local soil. However, as with the recovery of the count rate following the Forbush decrease, this is unlikely to be on a short enough timescale to significantly affect the prominence of the peak coincident with GLE72. Also, similar levels of rainfall were recorded in the vicinity of most of the other COSMOS stations, without this leading to a spike in the count rate coincident with GLE72.

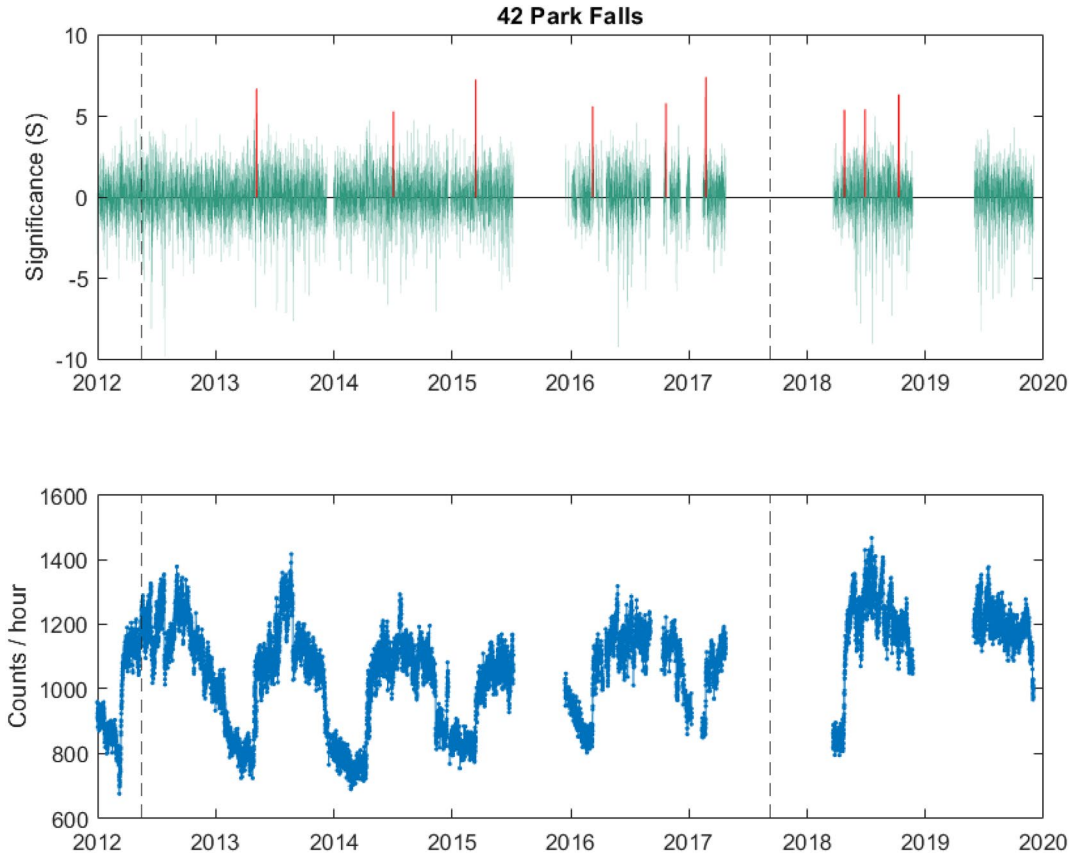

Figure 12. Park Falls COsmic-ray Soil Moisture Observing System detector count rates in 4-h binning scheme (lower panel) with corresponding value for significance S (upper panel). Ground level enhancement (GLE71) and GLE72 are represented by dashed vertical black lines. Red lines in the S data series are used to highlight instances where $S > 5$.

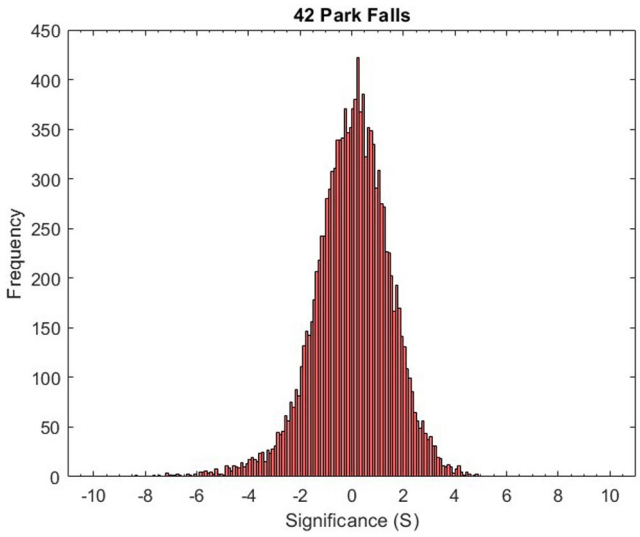

Figure 13. Histogram of calculated *S* values for Park Falls.

One further consideration when considering the value of S in the Barrow data at GLE72 ($S = 6.9$) is the systematic uncertainty in the data caused, primarily, by local soil moisture effects. We have defined significance ("S") using Poisson statistics based on the count rate over the previous 24 h (where $\bar{\sigma}_P$ in Equation 1 is effectively an estimator of the local count rate standard deviation). By fitting the distribution of S at the Barrow site with a Gaussian function, we estimate that the standard deviation of the full count rate time series is systematically higher by factor of 1.14. Hence, instead of 6.9 $\bar{\sigma}_P$, the significance could be expressed as 6.0 σ_{tot}, where σ_{tot} includes a systematic error due to soil moisture effects. The longer timescale over which these effects occur could mean this is an underestimate of the significance of a localized peak in count rate, but either way it is clear that the statistical significance of the peak in the count rate at Barrow during GLE72 is high (though, as discussed above, the high prominence of the Barrow peak relative to Inuvik neutron monitor data suggests that to some degree that this is artificial). It is impossible to definitively determine how much, if any, of the excess counts in the Barrow data during GLE72 were a direct result of the event and how much are simply statistical fluctuation. Nonetheless, this example presents the best evidence we have found to date of a GLE signature in COSMOS data.

4. Theoretical Sensitivity to Historic and Future Events

The search for GLEs in existing COSMOS data is limited by their low occurrence rate in the brief history of the detector networks. However, we can examine the potential future usefulness of such networks via simulated events and consequent hypothetical count rate time series.

4.1. Atmospheric Environment Simulations

The starting point for simulating COSMOS detector count rates during potential GLE events is to define the primary proton spectra (defined as solar proton spectra incident at Earth before magnetospheric or atmospheric attenuation) for the hypothetical events of interest. Here we use both primary spectra derived from recent or prominent historical events, and also contrived spectra based on a parameterized spectral shape. The historical events we consider are listed in Table 4. Figure 20 shows primary (peak flux) spectra for the historical GLEs compared to a GCR background spectrum. Four of the peak flux spectra are derived from the total fluence spectra of Allan Tylka (Tylka, 2008) and are embedded in the MAIRE model (Hands et al., 2017), the remaining two are based on fits of the GLE71 and GLE72 by Alexander Mishev (Mishev et al., 2014; Mishev & Usoskin, 2018), excluding the pitch angle distribution factor. In all cases the GLE spectra are far softer than the GCR spectrum, though there is considerable variation in spectral shape between the GLEs.

To test the impact of spectral shape in a more controlled way, we also use contrived primary proton spectra using a simplified version of the power law in rigidity used by Mishev:

$$J(P) = J_0 P^{-(\gamma + 0.3x(P-1))} \tag{2}$$

Where P is the rigidity, γ is the spectral index, and J_0 is a normalization factor for omnidirectional intensity, arbitrarily set at 100 protons/cm^2/s/sr/GV. The normalization value is unimportant as our interpretations of these spectra are based on *relative* impacts at different rigidities or altitudes, rather than absolute fluxes or count rates. Figure 21 shows five such spectra (converted to functions of energy) with γ ranging from 3 to 7, alongside a background GCR spectrum.

All spectra plotted in Figures 20 and 21 were used as inputs to the Model for Atmospheric Ionising Radiation Effects (MAIRE), which uses Monte Carlo radiation transport simulations to calculate the atmospheric radiation environment at all geographic coordinates and altitudes up to 20 km (Hands et al., 2017). MAIRE is capable of calculating differential and integral spectra for all major particle species, however for this task

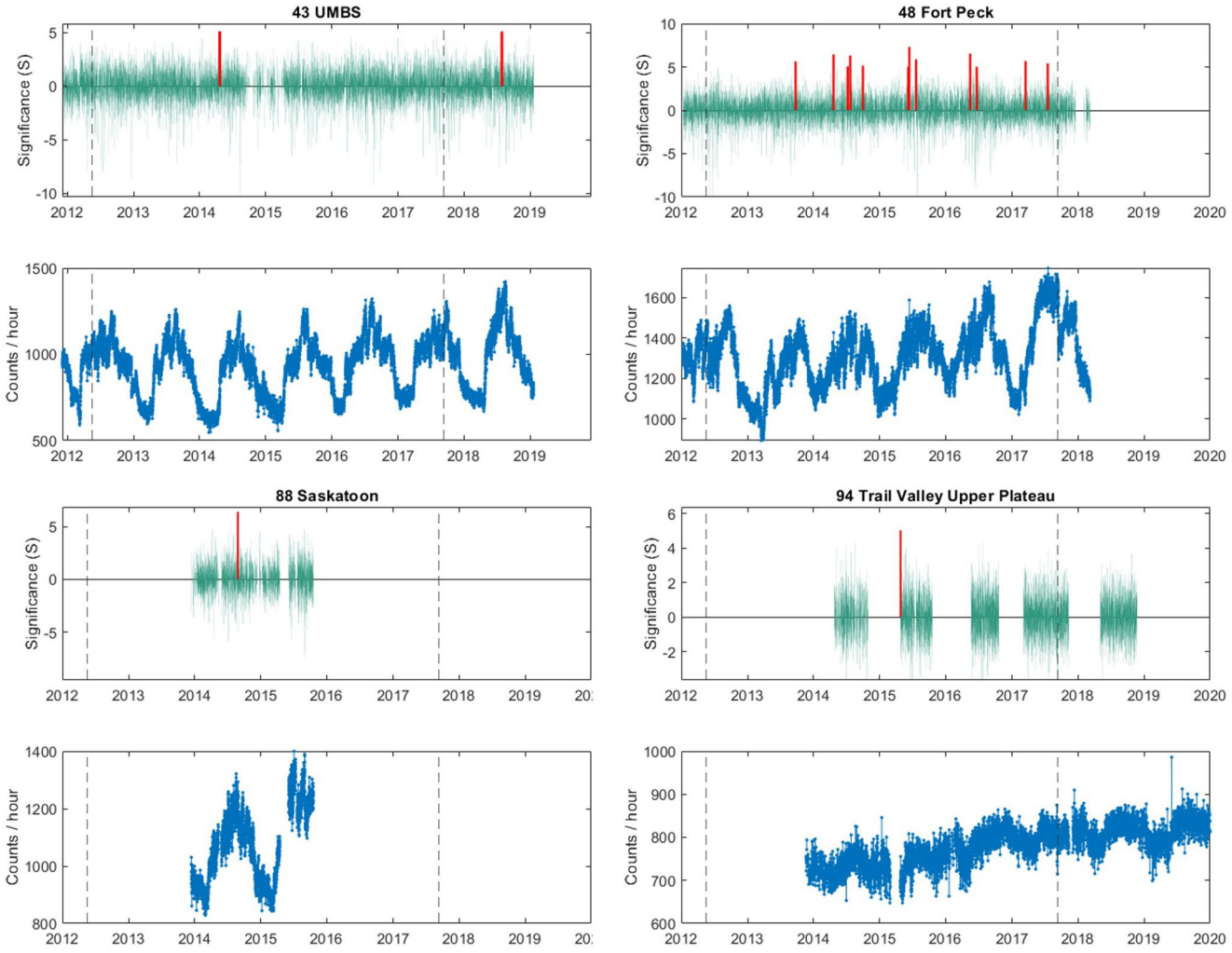

Figure 14. COsmic-ray Soil Moisture Observing System detector count rates in 4-h binning scheme (lower panel) with corresponding value for S (upper panel). Ground level enhancement (GLE71) and GLE72 are represented by dashed vertical black lines. Red lines in the S data series are used to highlight instances where $S > 5$.

we only require neutron flux. For a particular input primary spectrum, the two key determinants of the neutron spectrum are altitude and cut-off rigidity, and MAIRE further splits the output into upward and downward directions. Figure 22 shows downward differential neutron spectra at ground level and zero cut-off rigidity for each historical event shown in Figure 20.

The neutron spectra in Figure 22 show that the intensity of several of the historical events are comparable to the GCR background across a wide energy range at zero cut-off rigidity (top panel). GLE72 (10-Sep-17) and GLE05 (23-Feb-56) are notable as respectively being significantly less or more intense than the other events and the GCR background. The event which occurred on 23-Feb-56 (GLE05), is the largest event ever directly measured (Belov et al., 2005; Copeland & Atwell, 2019; Winckler, 1956). The GCR background spectrum exceeds all GLE events at the highest neutron energies (>10^4 MeV) because of the much harder primary proton spectrum. Similar spectra at two higher rigidities ($R = 2$ GV and $R = 4$ GV) are also shown in Figure 22. The higher rigidity causes the ground level neutron spectra to separate from each other due to the divergence of primary proton spectra at higher energies. The relative intensity of the GCR background also increases at higher rigidity as the relatively large number of soft (lower energy) protons in the GLE spectra are prevented from reaching the upper atmosphere by the magnetic field.

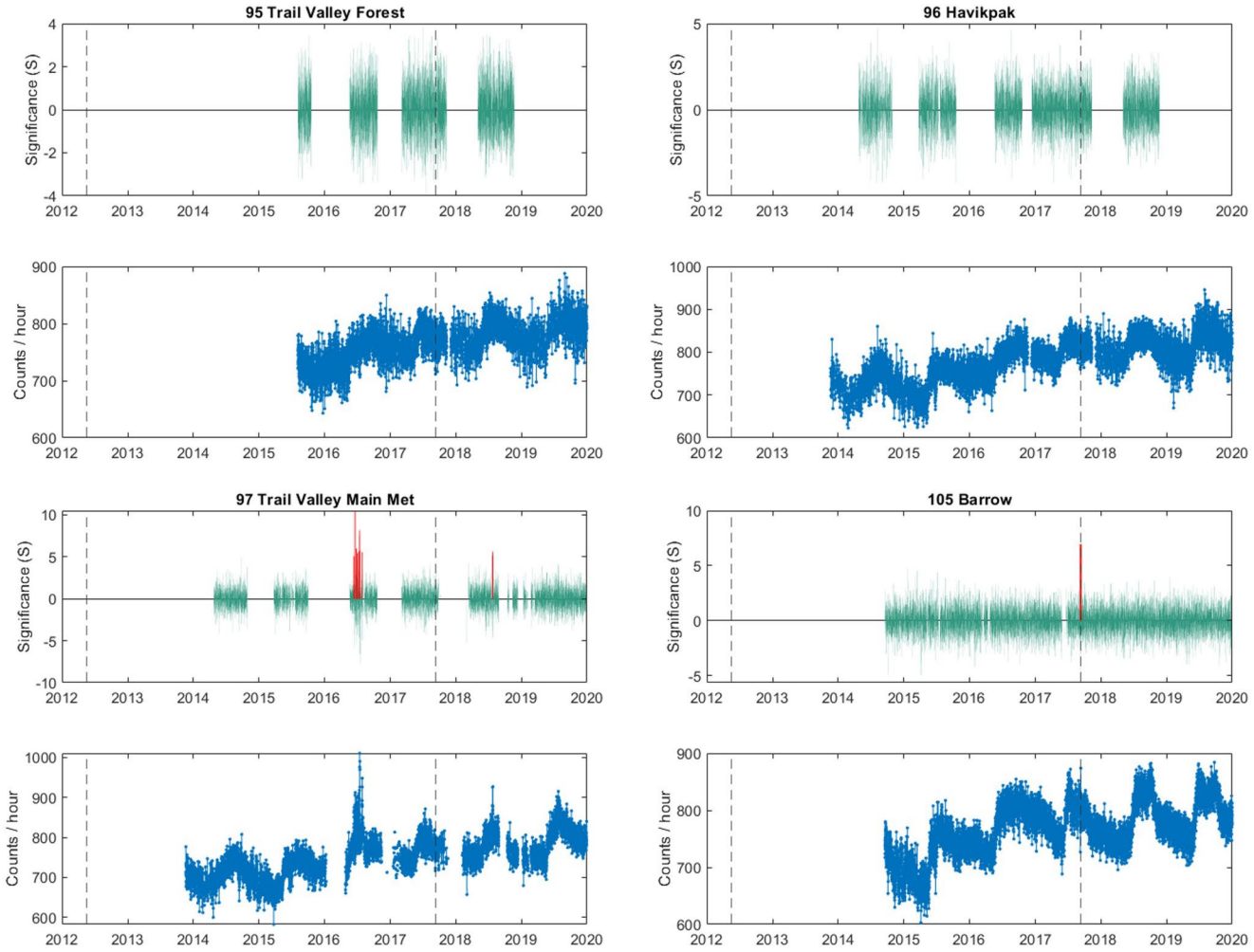

Figure 15. COsmic-ray Soil Moisture Observing System detector count rates in 4-h binning scheme (lower panel) with corresponding value for *S* (upper panel). Ground level enhancement (GLE71) and GLE72 are represented by dashed vertical black lines. Red lines in the *S* data series are used to highlight instances where $S > 5$.

Table 3
Summary of Calculated S Values at Each GLE Time and the Number of Occasions Where S > 5

Site ID	Name	*S* (GLE71)	*S* (GLE72)	#*S* > 5
42	Park Falls	2	-	11
43	UMBS	1.7	2.3	2
48	Fort Peck	3.4	3.5	12
88	Saskatoon	-	-	1
94	TV UP	-	2.8	1
95	TV Forest	-	1.3	0
96	Havikpak	-	2.4	0
97	TV Main Met	-	1.7	13
105	Barrow	-	6.9	1

Abbreviation: GLE, ground level enhancement.

Figure 23 shows downward neutron spectra at ground level for the five contrived GLE spectra at the same three cut-off rigidities as above ($R = 0$, $R = 2$, and $R = 4$ GV). As the normalization of these primary input spectra is arbitrary the relative intensity between the events of different spectral index and compared to the GCR background is unimportant. However, the effect of rigidity on the relative intensity is very clear, as is the apparent similarity between the shapes of the ground-level neutron spectra, regardless of primary spectral index and cut-off rigidity. As will be demonstrated later, this latter observation greatly simplifies the interpretation of the effect of shape of the primary spectra on COSMOS detector count rates.

A common way of comparing atmospheric neutron spectra is to plot the flux per lethargy (the natural logarithm of the energy) against energy on linear-log axes, such that equal areas under the curve represent equal neutron flux. Figure 24 shows two examples of historical events compared to the GCR background in flux per lethargy format. GLE59 (July 2000) has a much softer primary spectrum than GLE05 (February 1956), however this has a negligible effect on the shape of the secondary neutron spectrum. In relative terms, the main difference between these

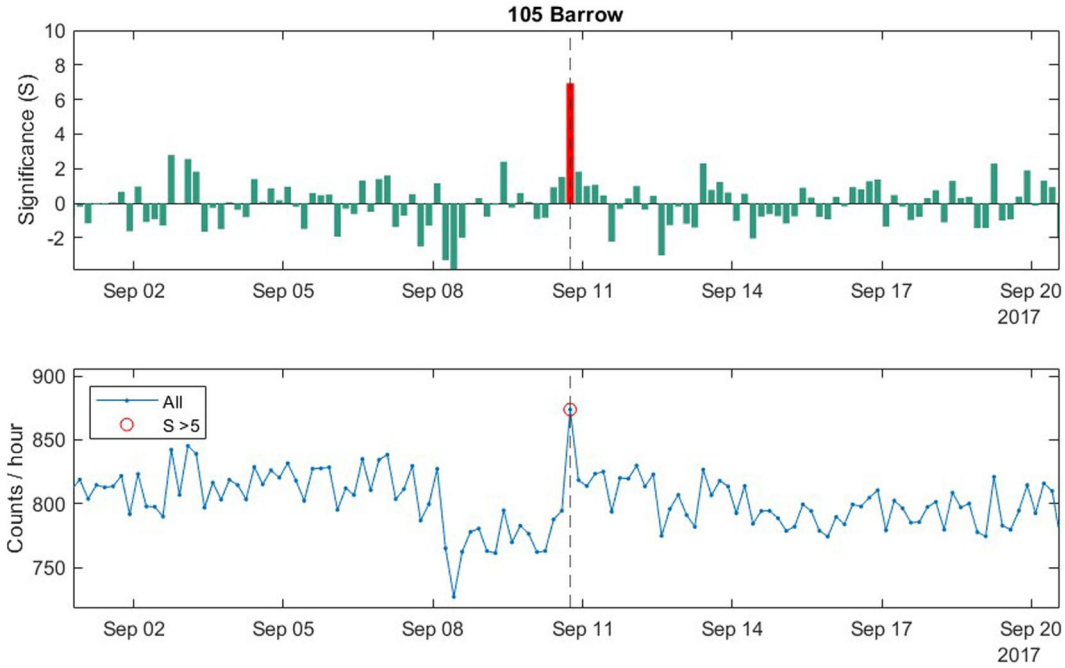

Figure 16. Barrow COsmic-ray Soil Moisture Observing System detector count rates in 4-h binning scheme (lower panel) with corresponding value for S (upper panel) in September 2017. Ground level enhancement (GLE72) is represented by a dashed vertical black line. Red indicates $S > 5$ in both panels.

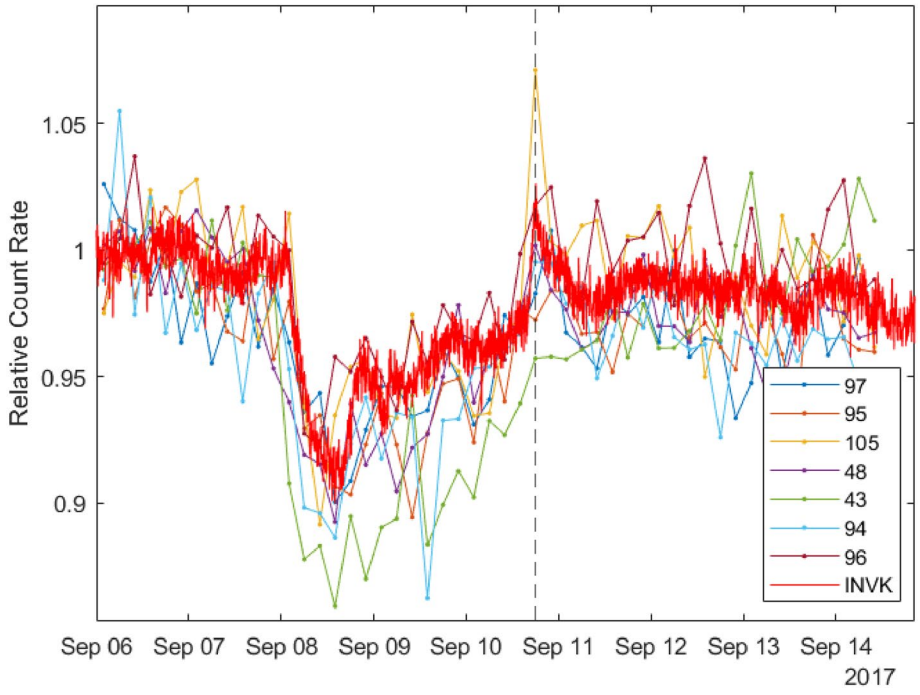

Figure 17. Renormalized COsmic-ray Soil Moisture Observing System data from seven stations during ground level enhancement (GLE72) in September 2017 (lines with dotted points). Equivalent renormalized count rates from the Inuvik (INVK) neutron monitor station are also plotted (red line). GLE72 is represented by a dashed vertical black line.

Figure 18. Map showing the relative locations of some of the low rigidity COsmic-ray Soil Moisture Observing System stations and the Inuvik (INVK) neutron monitor station. The color scale of location circles indicates rigidity cut-off.

spectra and the GCR background is seen at very high energies where the ratio between GCR and GLE neutron flux increases substantially. However, as the fraction of neutrons in this part of the spectrum is small even for GCR, the impact is limited.

4.2. URANOS Simulations

The URANOS Monte Carlo code (Köhli et al., 2015) is designed to allow the rapid modeling of neutrons in the ground and lower atmosphere in order to address questions in environmental science. The

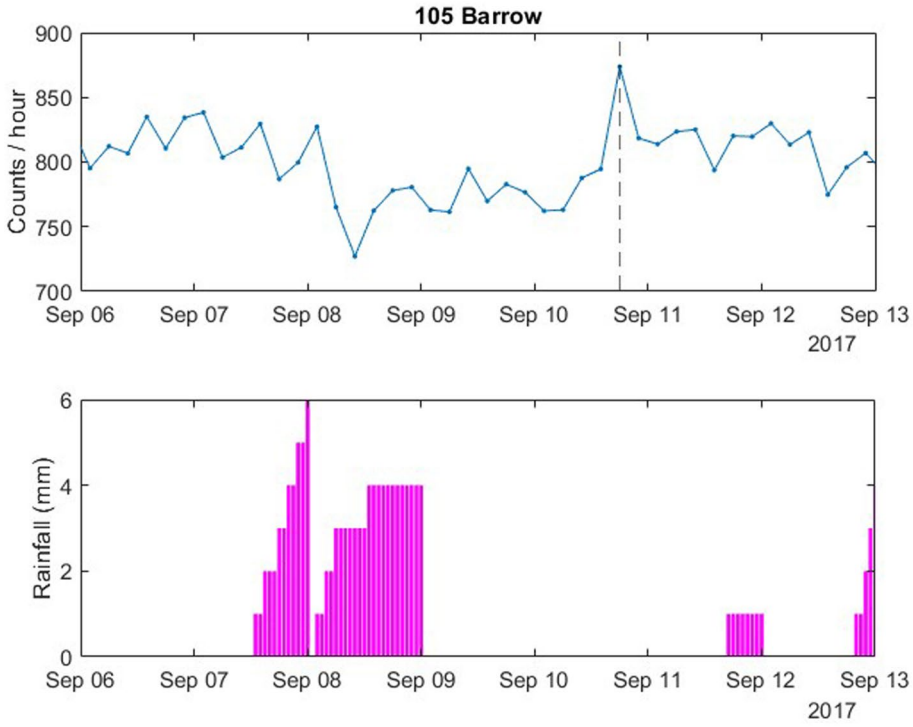

Figure 19. COsmic-ray Soil Moisture Observing System Barrow count rate (upper panel) in 4-h bins compared to ERA5-Land hourly rainfall data (lower panel) from a 9 km grid resolution. Ground level enhancement72 is represented by a dashed vertical black line.

Table 4
List of Historical GLEs Used in This Analysis

Reference	Date
GLE05	February 23, 1956
GLE42	September 29, 1989
GLE59	July 14, 2000
GLE60	April 15, 2001
GLE71	May 17, 2012
GLE72	September 10, 2017

Abbreviation: GLE, Ground level enhancement.

representation of the soil in this model allows soil moisture to be easily changed. For typical applications, neutrons are injected into URANOS at very low altitudes (50–80 m) using an input spectrum designed to reproduce measured/simulated ground-level spectra after the neutron collisions simulated within URANOS itself have been accounted for. Here, we use URANOS to simulate the ground and lower atmosphere up to a height of 500 m, while MAIRE is used to simulate the propagation of neutrons in the upper atmosphere down to a height of 500 m. URANOS simulations are performed for both the historical and contrived GLE events with different rigidities and with several levels of soil moisture.

MAIRE downward neutron spectra at ground level and at 500 m altitude are shown in Figure 25 for the Feb-56 (GLE05) environment. At 500 m, the effect of ground interactions (which is present in the ground level spectrum) is negligible. The difference in the shape of the two spectra is most visible in the thermal neutron regime ($\sim 10^{-8}$ MeV) but there is also a significant difference in the epithermal energy range up to ~0.01 MeV. Because of this, all thermal neutrons and a significant fraction of epithermal neutrons in the resulting ground level spectra local to COSMOS detectors will be produced in the URANOS simulations rather than by MAIRE. A suitable input spectrum for URANOS is obtained by selecting the downwards moving neutrons from the MAIRE spectra at 500 m, while the atmosphere within URANOS is terminated above 500 m. Therefore, any neutron that leaves the URANOS simulation domain (scatters above 500 m) will be removed. This prevents the double counting of neutrons (already simulated by MAIRE) that would occur if such neutrons where allowed to scatter back into the simulation domain. Each MAIRE input spectrum is used by URANOS to simulate interactions with the ground and calculate ground level neutron spectra as a function of rigidity and soil moisture. The five combinations of volumetric water content (VWC) and cut-off rigidity are summarized in Table 5. Three values of VWC at a common rigidity (2 GV) allows us to explore the effect of that parameter in isolation, and similarly three values of rigidity at a common VWC value (25%).

Omnidirectional ground level neutron spectra have been calculated by URANOS in the energy range 10^{-8}–2×10^4 MeV for the parametric combinations given in Table 5. Results for the background galactic cosmic ray environment were calculated using an input date of May 2016, which means solar modulation of the GCR environment is at a mid-level in between solar maximum and solar minimum. URANOS spectra for these input conditions are shown as flux per lethargy in Figure 26.

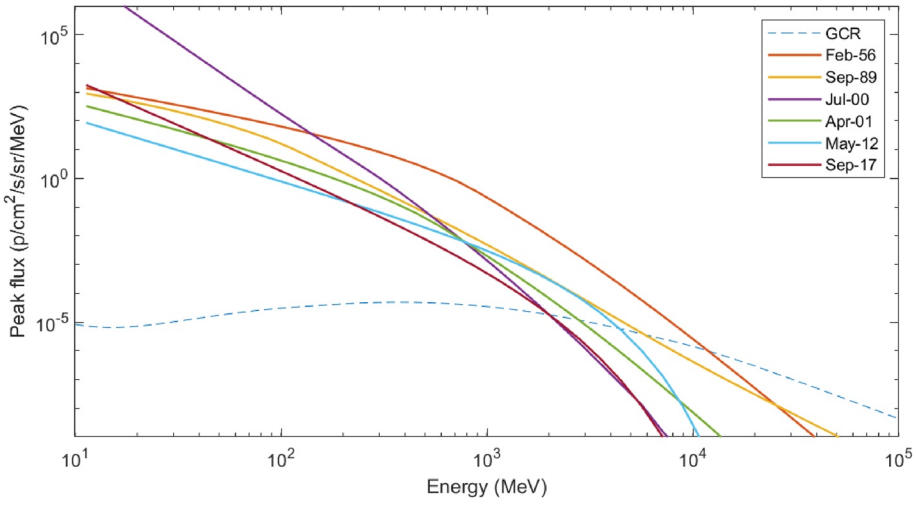

Figure 20. Peak flux energy spectra for six historical ground level enhancements. The background galactic cosmic ray spectrum is also shown for comparison.

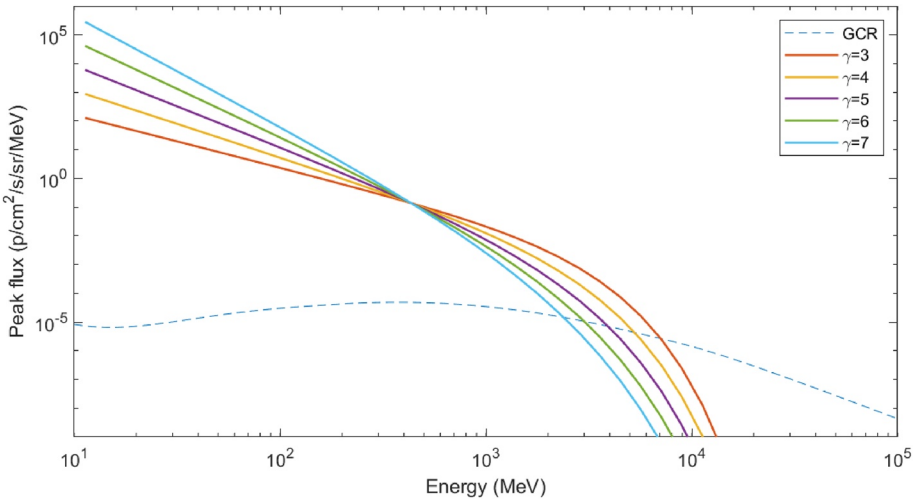

Figure 21. Peak flux energy spectra for five ground level enhancements with different spectral indices. The background galactic cosmic ray spectrum is also shown for comparison.

For a GCR spectrum the effect of cut-off rigidity on the ground level neutron spectrum is small (up to 4 GV). A much more significant VWC effect is visible, especially at the lowest value (5%) where the dryer conditions lead to less absorption and more reflection of the incident neutron spectrum by the ground layer. This is the well-known effect by which principle CRNS detectors are designed to operate for soil moisture measurement applications.

Figure 27 shows equivalent ground level spectra for the six historical GLEs. Although the cut-off rigidity influences the different events to different degrees, the effect is found to be much larger than for the GCR spectra (Figure 26), and also larger than the influence of soil moisture in all cases. This is due to the softer primary input spectra for GLEs, which leads to significant variation in the downward neutron spectrum at 500 m that serves as input to URANOS. Soil moisture influences the neutron spectra for energies approximately in the range 1 eV to 1 MeV. Proportionally, this influence has very little dependence on the historical event considered and is also approximately the same as that seen for GCR. The flux either increases by ~50%, or decreases by ~20%, as VWC is changed to 5% or 45% respectively (from a baseline of 25%). The same proportional change is expected regardless of rigidity and arises due to the similarity in the shapes of the secondary neutron flux (as depicted in Figure 23 as well as in Figure 27). The effect of the cut-off rigidity is illustrated even more clearly in Figure 28, which shows ground level neutron spectra for the contrived GLEs defined by spectral index parameter γ. As expected, the influence of the cut-off rigidity is strong for all events but is strongest for the softest event ($\gamma = 7$). The proportional effect of changing VWC is the same as for the historical events. Unlike conventional ground level neutron monitors (GLNM), which are most sensitive to the highest energy neutrons that display very little sensitivity to VWC, COSMOS detectors are, by design, particularly sensitive to the neutron energies most influenced by VWC.

4.3. COSMOS Count Rates

Ground level neutron spectra calculated by URANOS can be used to estimate CRNS (COSMOS) detector count rates by multiplication with an appropriate detector response function. The COSMOS detector response function is based on a CRS1000/B type (Köhli et al., 2018). GLNM response functions are dominated by high-energy neutrons because the neutron monitor design includes a lead producer that increases the number of local evaporation neutrons by more than an order of magnitude over the number of incident neutrons (Clem & Dorman, 2000). By contrast, the CRNS response is much more evenly distributed from the thermal to fast energy regimes, peaking at around 1 eV (10^{-6} MeV). It is lower energy neutrons (<10 MeV) that are most affected by scattering due to water molecules, which demonstrates why COSMOS detectors are sensitive to local soil moisture conditions, whereas neutron monitors are not.

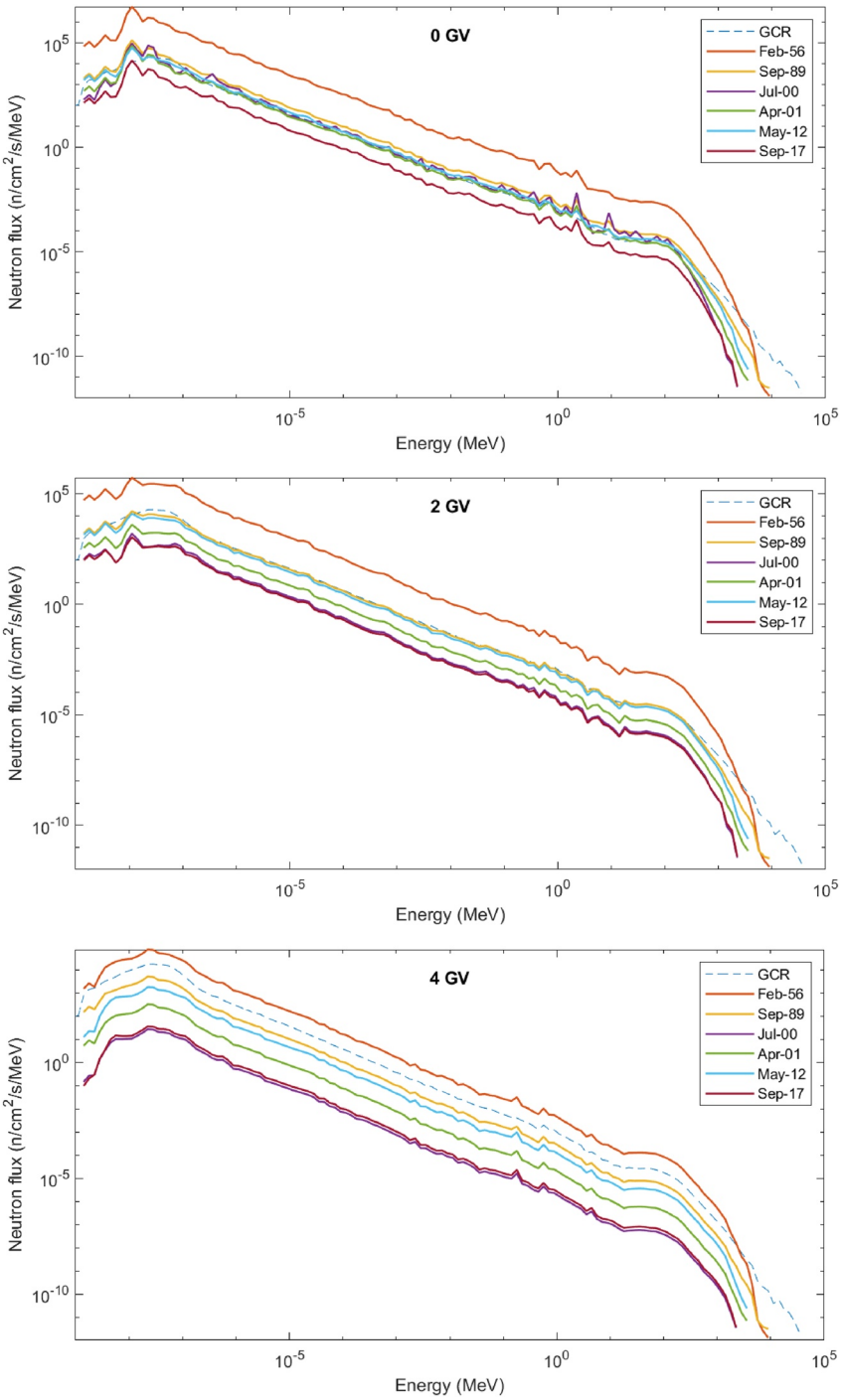

Figure 22. Ground level neutron spectra at $R = 0$ GV (top), $R = 2$ GV(middle), and $R = 4$ GV (bottom) for historical ground level enhancements and the GCR background. In each case the y axis is differential neutron flux in the downward direction.

Estimates of absolute count rate are made for GCR conditions and historical GLEs (contrived GLEs based on spectral index are excluded as the normalization is arbitrary). Figure 29 shows the estimated count rates for the GCR background spectra (at different cut-off rigidity and VWC combinations) and the equivalent count rate estimates for six historical GLEs (not inclusive of the GCR background). In all cases the effect

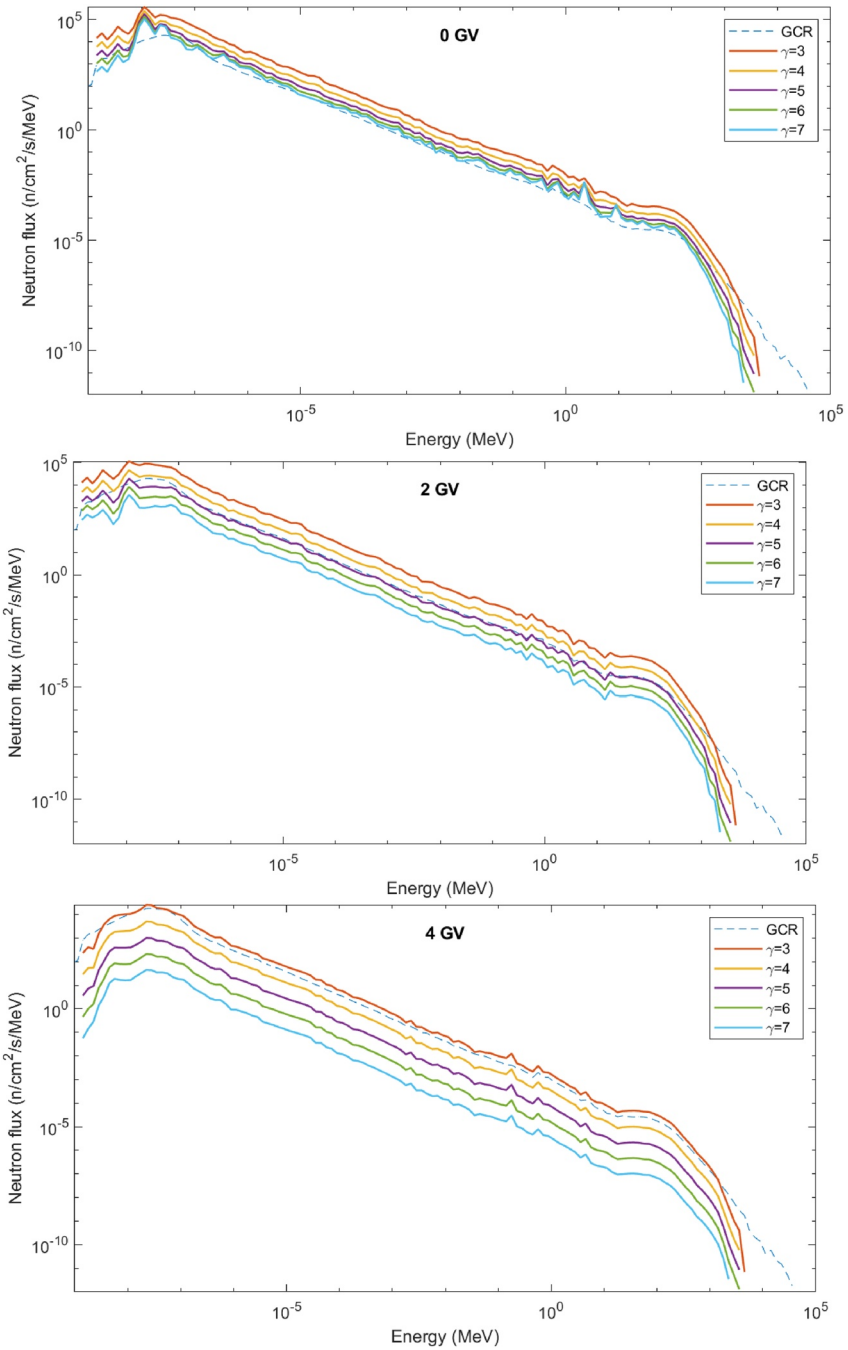

Figure 23. Ground level neutron spectra at $R = 0$ GV (top), $R = 2$ GV (middle) and $R = 4$ GV (bottom) for contrived ground level enhancement spectra as a function of spectral index and the GCR background.

of VWC is stable, that is, the ratio between count rates at 5%, 25%, and 45% VWC is independent of event spectrum.

These count rate estimates show both the enormous variation in impact between GLE events and the relative impact of rigidity compared to VWC. For a hypothetical GLE alert system it is also of interest to compare the relative increases of GLNM and CRNS type detectors. Figure 30 shows predicted percentage increases during GLE05 (Feb '56) for a GLNM detector (based on a 6-NM64 design), a CRNS detector and the >10 MeV neutron flux. The energy threshold is largely arbitrary due to the relative insensitivity of the shape

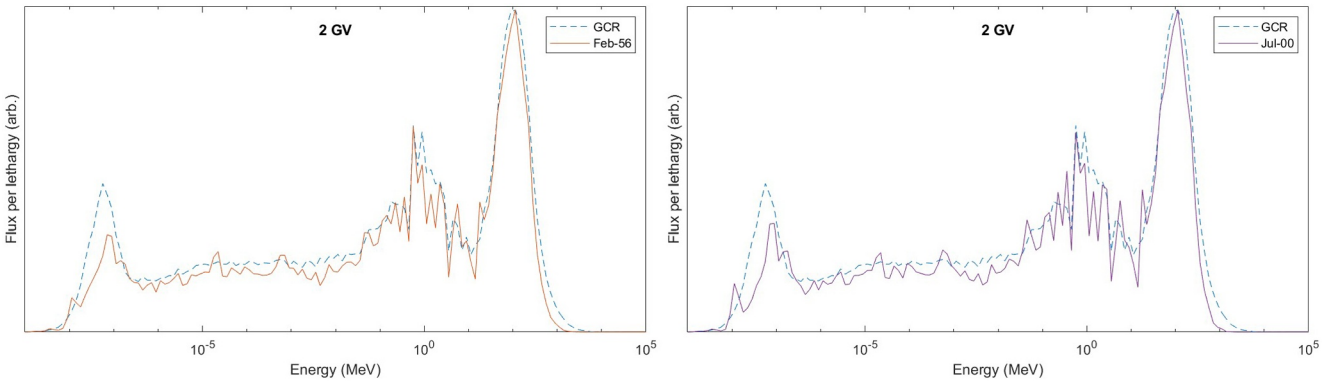

Figure 24. Flux per lethargy comparison of ground level GCR neutron spectrum at 2 GV with ground level enhancement (GLE05; LHS) and GLE59 (RHS). The *y* axes have been renormalized to compare the shapes of each curve and the units are arbitrary.

of ground neutron spectra to primary proton spectra. As this is a relative calculation (comparing to GCR background), even the CRNS increases are independent of VWC. Both >10 MeV flux and predicted CRNS count rate increase exceed the predicted count rate increase for GLNMs. This is entirely because the GLNM response function is so heavily skewed toward high energy neutrons. The apparently small difference in the high energy tail of the neutron spectra shown in Figure 24 is sufficient to mean that when the total neutron flux during a GLE increases by a factor, f, the increase in GLNM count rate is $<f$. However, the effect is small and, as can be seen in Figure 30, less significant at higher rigidities where the influence of softer protons in the primary GLE spectrum is reduced. In terms of statistical significance, the much higher baseline count rate of GLNMs (hundreds of times greater than a COSMOS detector) more than compensates for a slightly lower percentage increase. In the next section we explore how the statistical significance of hypothetical GLEs can be improved by increasing the baseline count rate of COSMOS detectors.

4.4. Theoretical Sensitivity to Future GLE Events

The utility of a hypothetical COSMOS-based GLE alert system depends on its capacity to detect increases in the ground level neutron flux. This, in turn, depends on the statistical significance of increases in count rate

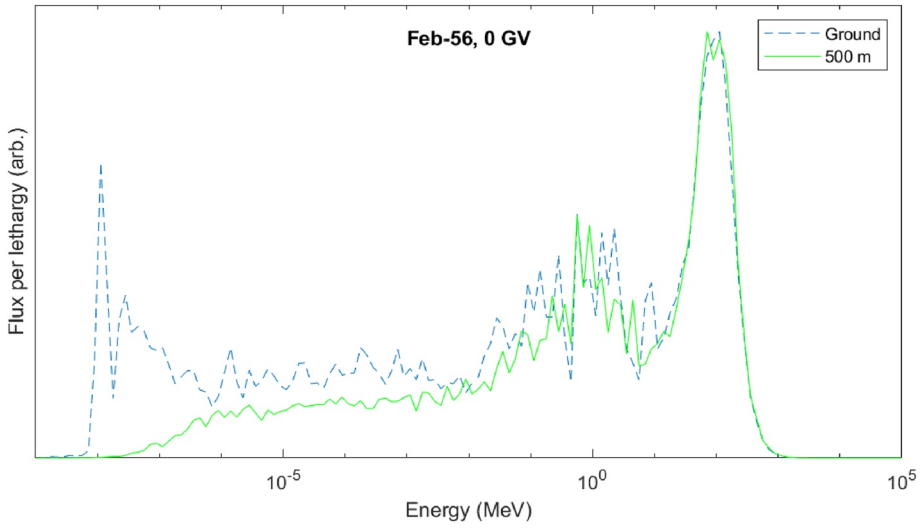

Figure 25. Downward flux per lethargy comparison of neutron spectrum for GLE05 (Feb '56) at ground level and 500 m altitude (both at zero cut-off rigidity). The *y* axes have been renormalized to compare the shapes of each curve and the units are arbitrary.

Table 5
Combinations of Soil Moisture and Rigidity Selected for Evaluating URANOS Ground Level Neutron Spectra

	Volumetric water content (VWC)		
Rigidity (GV)	5%	25%	45%
0		✓	
2	✓	✓	✓
4		✓	

relative to a baseline GCR rate. In this section we explore how statistical significance relates to the following event and detector parameters:

1. Event magnitude: Increase in count rate relative to baseline during peak of event.
2. Event time profile: The evolution of the intensity of the event with time.
3. Event spectrum: Primary spectral index and impact on count rate at different cut-off rigidities.
4. Detector number: Grouping many COSMOS detectors at a single site or aggregating data from individual detectors across many sites.
5. Detector time resolution: Cadence of recording/transmitting counts from each detector
6. VWC: Soil moisture content of local environment.

To simplify this analysis, we assume a baseline count rate of 1,500 counts per hour for a single COSMOS detector during background conditions and a 25% VWC value. We also assume that the effect of different VWC values is fixed and consistent with the ratios in Figure 29, which means baseline count rates of 2,325 and 1,245 counts per hour for 5% and 45% VWC respectively. Unless otherwise stated all plots assume 25% VWC as default.

4.4.1. Event Time Profile

The time profile of GLE events varies greatly not just from event to event but also between locations for a particular event. However, it is often possible to group events into two broad categories: impulsive events and gradual events (though in practice most events have elements of both). Impulsive events have a fast initial rise in ground level neutron flux, followed by a slower (but still relatively rapid) decline. These events are associated with active regions near the western solar limb, which are magnetically well-connected to the Earth (McCracken et al., 2008, 2012). Gradual events are associated with more central origins in terms of solar longitude, resulting in significantly longer rise and fall times (Shea & Smart, 1990). Figure 31 shows some examples of increases in ground level neutron monitor data for several events (including four of the six historical events we have considered above) where these two broad categories are identifiable by early and late peaks in relative magnitude for impulsive and gradual events respectively. The specific station of origin for the neutron monitor data in each case is unimportant as this figure is illustrative only.

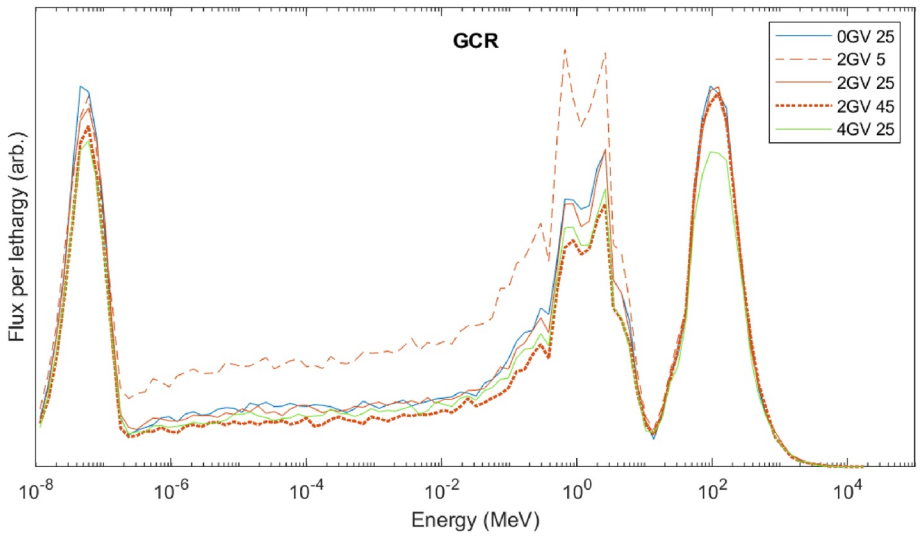

Figure 26. Ground level neutron spectra calculated by URANOS for GCR conditions, plotted as flux per lethargy with arbitrary *y* axis units. Blue, orange, and green colors show rigidity variation from 0 to 4 GV; dashed, solid and dotted lines show volumetric water content (VWC) variation from 5% to 45%.

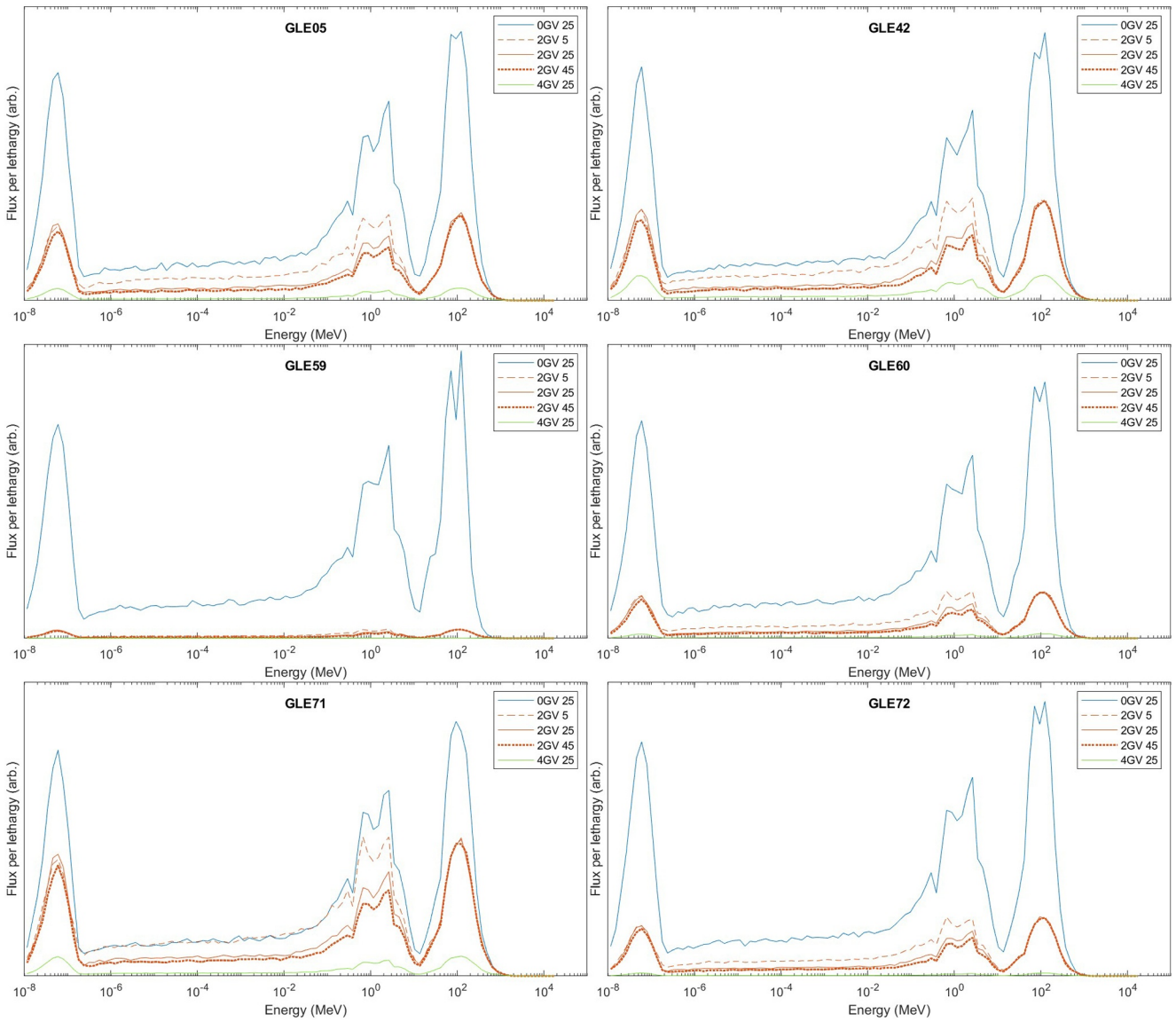

Figure 27. Ground level neutron spectra calculated by URANOS for historical ground level enhancements, plotted as flux per lethargy with arbitrary *y*-axis units (not consistent between plots). Blue, orange and green colors show rigidity variation from 0 to 4 GV; dashed, solid and dotted lines show volumetric water content (VWC) variation from 5% to 45%.

To recreate artificial time series of detector count rates we use contrived time profiles based on the exponential rise and fall times given in Table 6. The rise and fall times for an impulsive event are 2 and 30 min respectively (this is a very fast rise time but even faster have been reported by McCracken et al., 2016). The rise and fall times for a gradual event are significantly longer at 120 and 180 min respectively. The time profiles that result from these parameters are plotted in Figure 32.

The artificial count rates in Figure 32 (RHS) are based on a GLE with a peak magnitude at ground level that is equal to the cosmic ray background (thus a 100% increase and total count rate of 3,000 counts per hour). For this time series, and others to follow, the primary GLE spectrum does not need to be specified as we are defining the event magnitude relative to the baseline, regardless of location. This is a simplification because the primary spectrum is likely to change during the course of an event, although this is in part taken into account as the artificial time profiles are based on real events which themselves have time-dependent spectra.

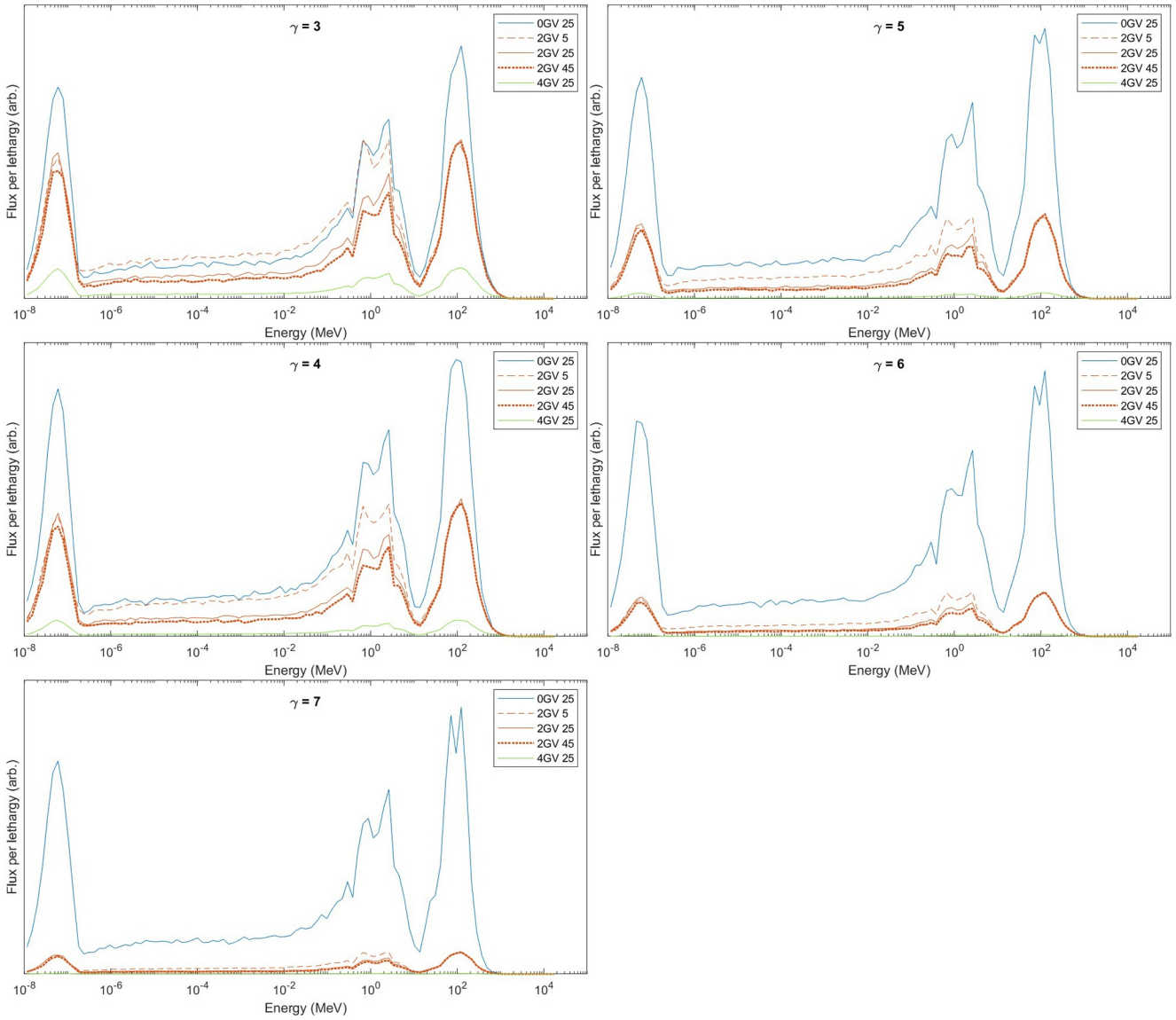

Figure 28. Ground level neutron spectra calculated by URANOS for contrived ground level enhancements of different spectral index (γ), plotted as flux per lethargy with arbitrary *y*-axis units (not consistent between plots). Blue, orange, and green colors show rigidity variation from 0 to 4 GV; dashed, solid and dotted lines show volumetric water content (VWC) variation from 5% to 45%.

4.4.2. Detector Time Resolution

Typical COSMOS time resolution currently stands at 60 min for the North American network and 30 min for the UK network. This compares unfavorably to neutron monitors where the resolution is as fine as 1 min. Although a basic trade-off exists in theory between statistical significance and time resolution—higher accumulation time results in more counts per bin and thus lower statistical error—in practice there are few drawbacks to considering improving the time resolution capability of the operational detectors in the COSMOS-UK network: while this may increase data transfer costs, it also widens the network's application scope. For soil moisture applications, data can always be re-binned after they are accumulated, thereby avoiding impacts on statistical significance for this application. Meanwhile, a higher time resolution can better support space weather applications, as we show here—and statistical significance here can be addressed by aggregating across detectors, as we discuss in the next section.

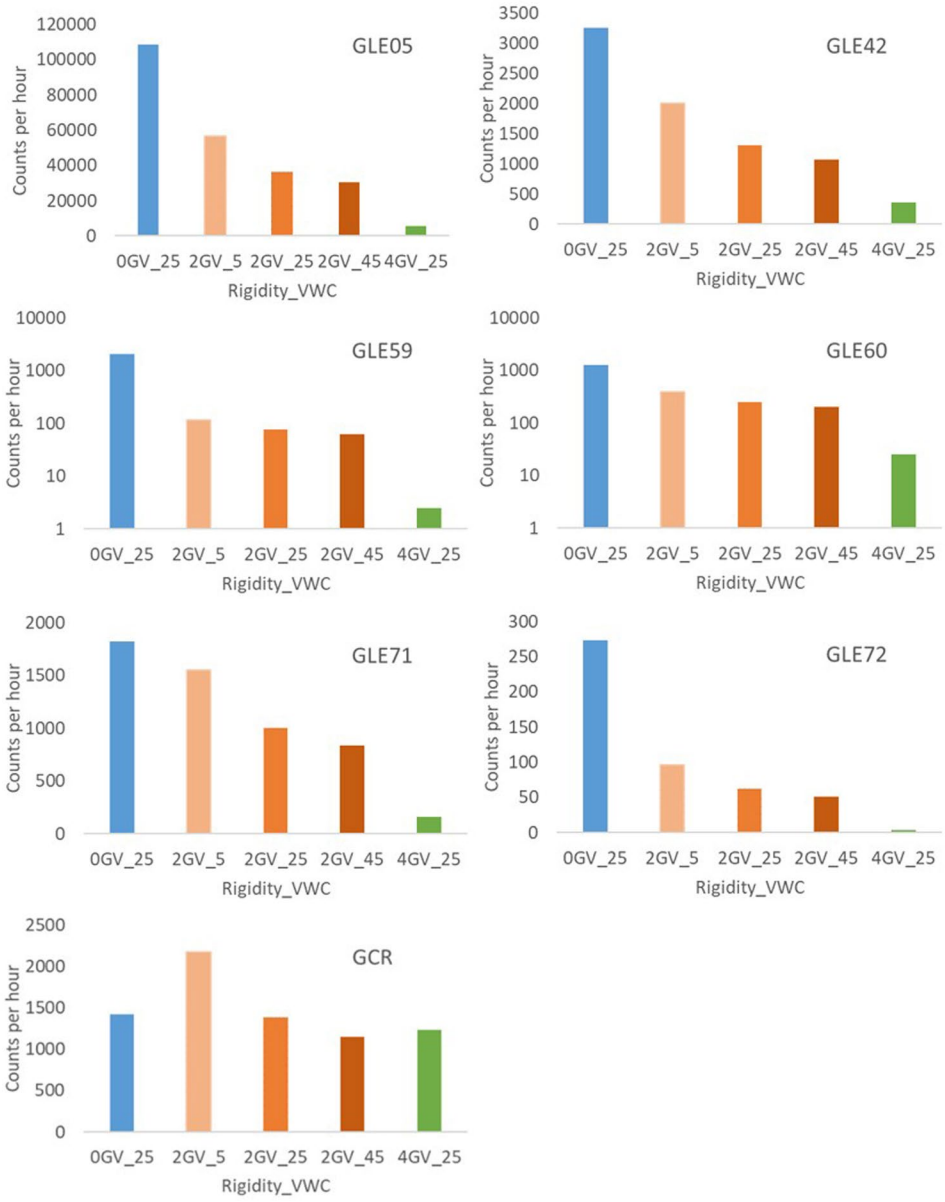

Figure 29. Estimates of cosmic ray neutron sensor count rate for six historical ground level enhancements (GLEs) and GCR background at different cut-off rigidity (#GV) and volumetric water content (_#%). GLE charts shows additional count rates above the GCR background rates. GLE59 and GLE60 are shown on a logarithmic scale, all others on a linear scale. Blue, orange, and green colors show rigidity variation and shades of orange show volumetric water content variation.

The impact of time resolution on the measured profile of different types of GLE can be seen in Figure 33. For a gradual event profile, even a 60-min counts-binning scheme is sufficient to resolve the profile of the event. By contrast, for an impulsive event such a coarse resolution results in the peak magnitude of the event being underestimated by nearly a factor of two. Fifteen minute resolution results in a smaller underestimate of ~13% but the profile of the rise time is missed entirely. This principle applies to all examples of count rate time series and statistical significance that follow.

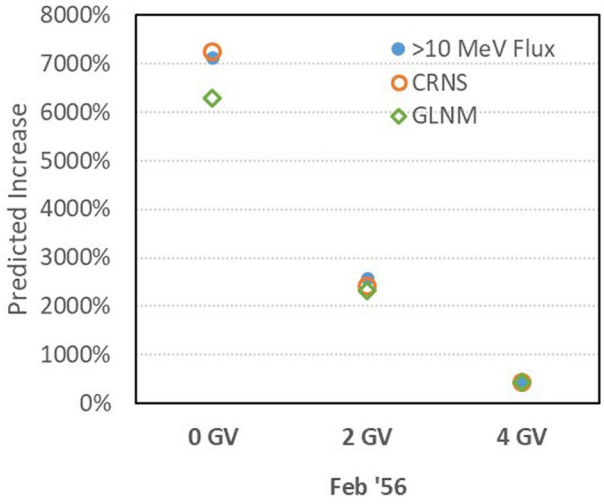

Figure 30. Predicted increase of ground level neutron monitor count rate, cosmic ray neutron sensor count rate and >10 MeV neutron flux during GLE05.

4.4.3. Statistical Significance

In our examination of existing COSMOS data during recent GLEs we applied a simple test based on Poisson statistics to evaluate the significance of any observed data spikes. We apply the same basic principle here to test the significance of hypothetical count rate increases during possible future events. We define one standard deviation, σ, as the square root (Poisson error) of counts in a single time bin during the quiescent (baseline) period prior to the event (e.g., $\sigma = \sqrt{1{,}500} = 38.7$ for 60-min resolution and 25% VWC). In all examples that follow, significance (#σ) is applicable to each individual time bin relative to baseline, rather than a post-event analysis of the overall significance of a well-resolved complete event profile. Also, given the many possible combinations of event magnitude, event time profile, detector time resolution, detector number and VWC, we present the following three examples based on impulsive and gradual GLEs each with a 10% increase at peak:

1. Single COSMOS detector, 25% VWC, variable time resolution (1–60 min)
2. 15-min resolution, 25% VWC, variable #detectors with aggregated counts (1–100)
3. Single COSMOS detector, 60-min resolution, variable VWC (5%–45%)

Figures 34–36 show impulsive and gradual event time profiles of the value of significance for these three examples. For events of greater magnitude, the values can simply be scaled linearly (i.e., for an event with 100% increase at peak, all plotted significance values would be 10 times higher). Peak significance as a function of time resolution scales as the square root of bin size (with the caveat that the peak of impulsive events is blurred at coarse resolution and the significance reduces accordingly), as does peak significance as a function of detector number. This is intuitive in both cases as increasing bin size or detector number increases accumulated counts for both baseline GCR and GLE. The effect of VWC is more subtle as dryer conditions lead to small increases in both baseline count rate and GLE count rate, leading to an even smaller effect on significance. However, these examples clearly show how the significance of a GLE at its peak is highly dependent on a number of independent factors.

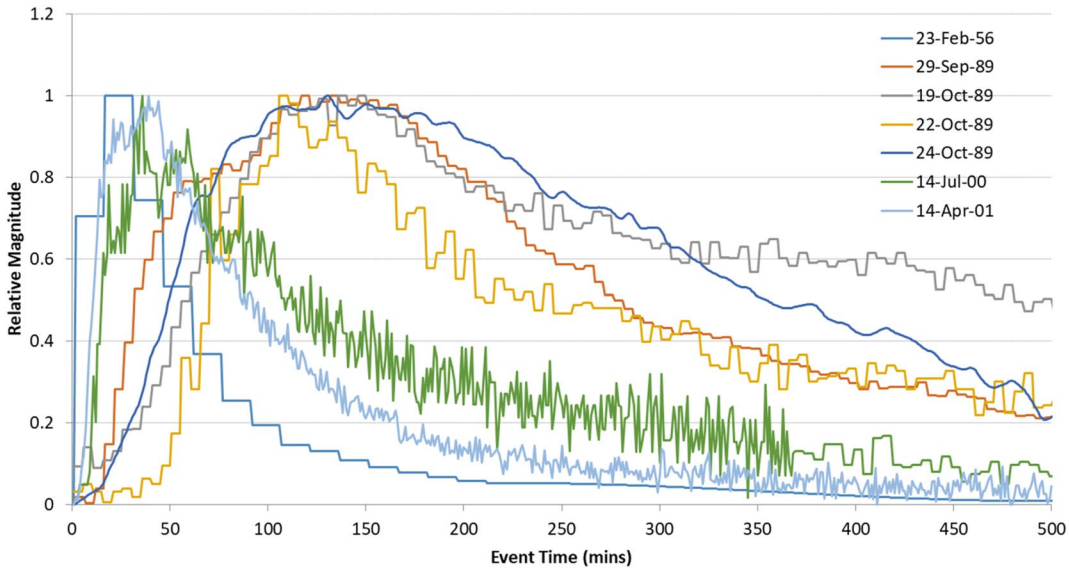

Figure 31. Examples of ground level enhancement time profiles based on neutron monitor data.

Table 6
Rise and Fall Times (in Minutes) of Artificial Time Profiles for Impulsive and Gradual Events

	Rise time	Fall time
Impulsive	2	30
Gradual	120	180

4.4.4. Detection Threshold

As shown in Figure 35, achieving high statistical significance during a GLE is aided greatly by aggregating the data from a number of COSMOS detectors. Whether these detectors should be co-located is a separate consideration and depends to some extent on the impact of rigidity variation. To consider how many detectors should be considered for aggregation it is helpful to quantify the effect this has on the capability for event detection as a function of event magnitude. For a very large event a small number of detectors, or even a single detector would be sufficient, however our analysis of real COSMOS data has shown that this is not the case for smaller events.

Figure 37 shows the relationship between event magnitude (at peak) and the number of detectors required to record a 5σ significance detection at a particular time resolution. For example, with our baseline assumptions a single detector is sufficient to measure a GLE peak of 100% magnitude with 1-min time resolution. However, for an event that produces only a 17% increase at its peak (like GLE71 at the Apatity neutron monitor), data from more than 30 detectors would need to be aggregated for the increase to reach 5σ significance. This number decreases to only two detectors with 60-min binning, and for a gradual event even just a single detector would be sufficient at this resolution.

4.4.5. Rigidity and Spectral Index

If we assume that the baseline case of 1,500 counts per hour during GCR conditions applies to a rigidity of 2 GV and VWC of 25% we can use spectral index to explore the relative effect of GLEs at different rigidities. For example, an event that causes a 10% increase in the ground level count rate at high rigidity would be expected to cause a significantly larger increase at low rigidity, and the margin of difference must depend on the primary GLE proton spectrum. Figure 38 (LHS) shows expected increase in count rate as a function of spectral index for $R = 0$ GV and $R = 4$ GV, during an event that caused a peak increase of 10% at $R = 2$. This relative comparison removes the arbitrary normalization applied to our contrived GLE spectra in Figure 21.

Using this relationship, it is theoretically possible to use data from two stations at different rigidities to infer the spectral index of the primary GLE spectrum that is the common cause of increases at both locations. For example, Figure 38 (RHS) shows two examples of the ratio of count rate increase as a function of spectral increase. For example, if an increase in count rate at a location corresponding to $R = 2$ GV were 10 times lower than a coincident increase at a higher latitude location with $R = 0$ GV, this would imply a spectral index of $\gamma = 7$. This is, of course, a simplification as there are several factors that complicate this relationship: spectral shape, longitudinal anisotropy, local soil moisture conditions, changes to cut-off rigidity during a geomagnetic storm etc. Nonetheless, the principle of using rigidity to infer spectral information during a GLE is well established by neutron monitors, and the UK spans a suitable rigidity range for a pair (or more) of detectors to be used for this purpose.

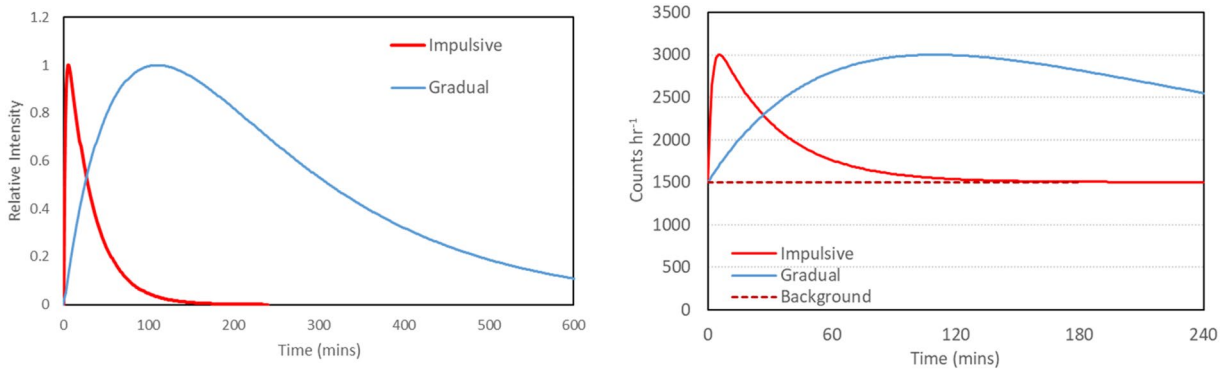

Figure 32. (LHS) Impulsive and gradual ground level enhancement (GLE) time profiles based on exponential rise and fall times. (RHS) Example of artificial count rate time series using these time profiles with a GLE resulting in a 100% increase at peak and a baseline count rate of 1,500 counts per hour.

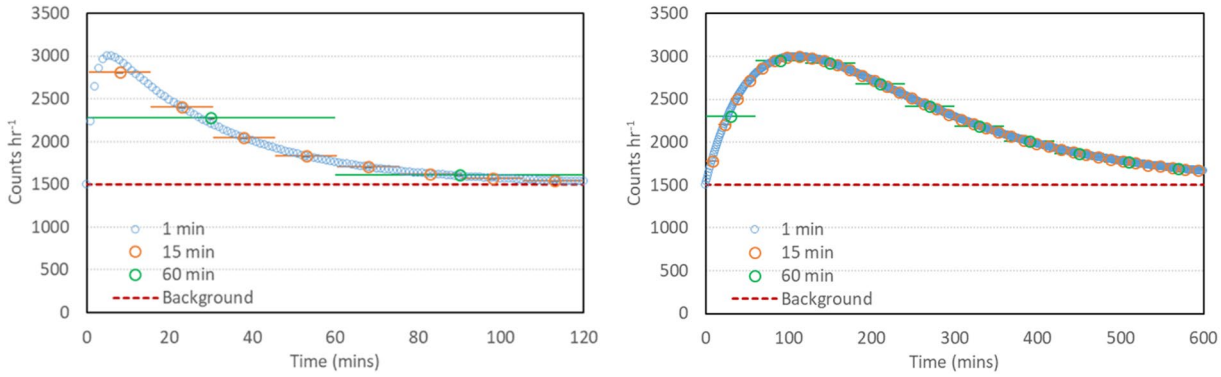

Figure 33. Artificial count rates at different time resolutions for an impulsive ground level enhancement (GLE) (LHS) and a gradual GLE (RHS) that result in a 100% increase at peak. 1-, 15-, and 60-min resolution are represented by blue, orange, and green circles respectively.

4.4.6. Terrestrial Gamma-Ray Flashes

As well as helping with space weather applications, increasing the time resolution of the COSMOS-UK soil moisture network may also support a second dual-purpose application: detection of terrestrial gamma ray flashes (TGFs), elevated atmospheric neutron fluxes from non-cosmic sources which have also been theorized and observed. TGFs in storm clouds can occur when electrons are excited to extremely high energies, leading to very short bursts of bremsstrahlung radiation with photon energies extending up to 10s of MeV (Dwyer et al., 2012). It is postulated that this primary gamma spectrum can result in significant photonuclear production, leading to short bursts of neutron fluence that are detectable at ground level. Observational evidence is plentiful for the gamma ray signatures of TGFs, especially from satellite-based instruments (Dwyer et al., 2010). Evidence for neutron fluences is far more limited, in part due to the highly localized nature of ground level neutrons from low altitude TGFs (Carlson et al., 2010), but also due to the extremely rapid nature of the events. The timescale of particle acceleration in TGFs is of the order of 1 ms or below (Babich et al., 2008), which means a large but very brief increase in the ambient neutron flux would not necessarily be seen by a detector with a significantly larger integration time. TGF neutrons should be distinguished from elevated neutron flux from so-called "gamma glow" events, which extend over much longer periods of time (seconds to minutes). For example, in September 2009 the Aragats neutron monitor in Armenia observed a ~3% increase in count rate that was sustained for several minutes and coincident with increased electron and gamma radiation seen in detectors on the same site during a thunderstorm (Chilingarian et al., 2010). Although this event cannot have been due to a TGF, recent observations and simulations have shown that TGFs and gamma ray glows may be directly related (Wada et al., 2019).

An example of a possible direct measurement of TGF-induced neutrons at ground level can be found in Martin and Alves (2010). During a lightning storm in January 2009 in Sao Jose dos Campos, Brazil, a thermal

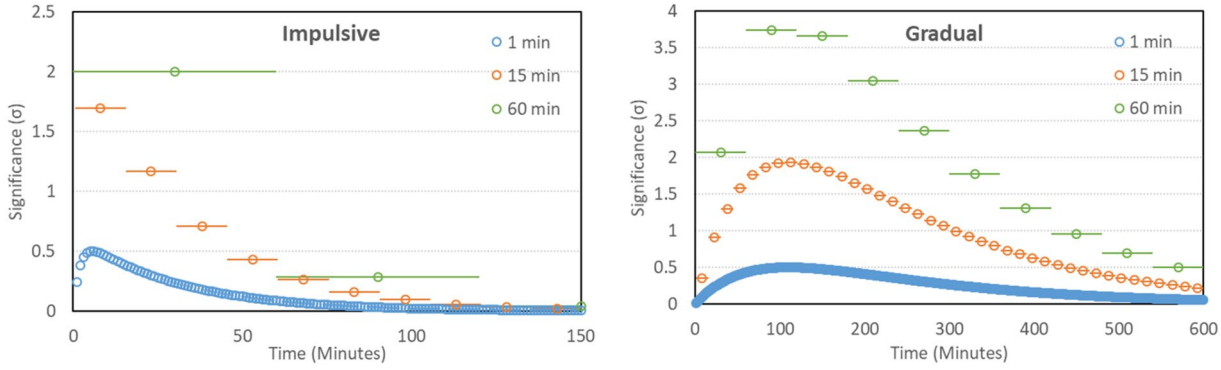

Figure 34. (Example 1) Time profile of statistical significance (per time bin) of a ground level enhancement with 10% peak magnitude relative to GCR, for a single COsmic-ray Soil Moisture Observing System detector and 25% volumetric water content.

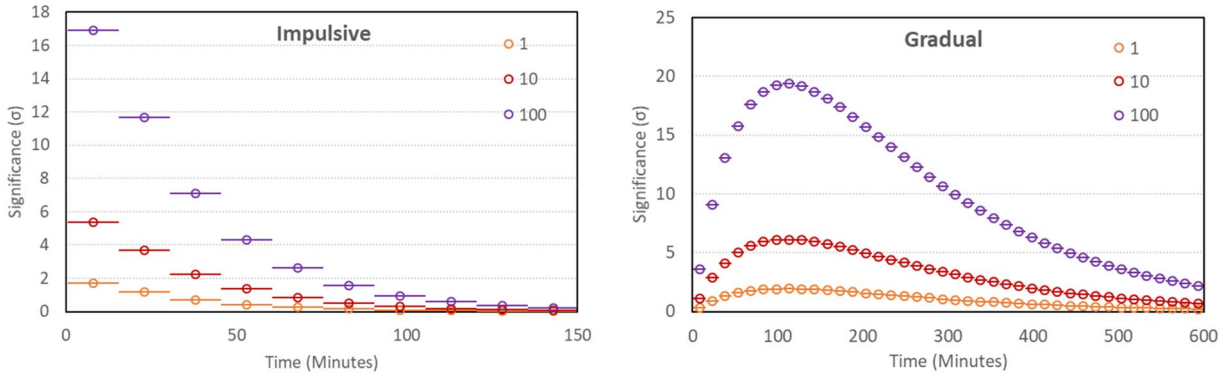

Figure 35. (Example 2) Time profile of statistical significance (per time bin) of a ground level enhancement with 10% peak magnitude relative to GCR, for a number of COsmic-ray Soil Moisture Observing System detectors in aggregate (1–100), 25% volumetric water content and 15-min time resolution.

neutron detector recorded a ~900 fold increase in count rate (Martin & Alves, 2010). However, as the time resolution of the detector was 1-min, this increase was recorded as 690 counts in a single bin (compared to a mean rate of ~0.7 counts per minute). By estimating detector-to-source distance as less than 500 m based on the time between the observation of the lightning flash and hearing of the thunder, the authors estimate that 10^{12}–10^{13} neutrons were produced by the lightning discharge. While this is consistent with, or even lower than, other estimates of TGF neutron production, the authors do not attempt to take into account the relationship between the source neutron spectrum, the modified spectrum at the detector location and the detector response function. Neutron spectra modeled by Carlson et al. (2010) reveal that both the source neutron spectrum and modified ground neutron spectrum (in this case after passage through 2.5 km of atmosphere) have mean energies in the MeV range (see Figure 39). The thermal neutron detector located at Sao Jose dos Campos has a negligible response to the such neutrons, which means that a significant amount of thermalization is implicitly assumed for the additional counts to be consistent with TGF origin. As the neutron spectra modeled in Carlson et al. (2010) extend down to only 1 keV, this analysis does not provide a thermal to fast neutron flux ratio. However, we can use the Carlson ground level spectrum to make order-of-magnitude count rate estimates for both ground level neutron monitors and COSMOS detectors.

A neutron monitor of 6-NM64 design records 2,000–3,000 counts per n/cm^2 in the neutron energy range 1–10 MeV (Clem & Dorman, 2000). Carlson et al. (2010) predict 1 n/cm^2 at ground level for a TGF at 2.5 km altitude (NB in their simulations the neutron flux at ground level is negligible for a TGF altitude above 5 km). We estimate two thirds of neutrons in their spectrum to be >1 MeV, which implies up to 2,000 additional counts from a low-altitude TGF. This compares to a typical count rate for this type of monitor at an equatorial location of ~50 counts per second. So, a TGF might be equivalent to 40 s worth of additional counts, or a 67% increase at 1-min resolution. This would certainly be statistically significant, however, as

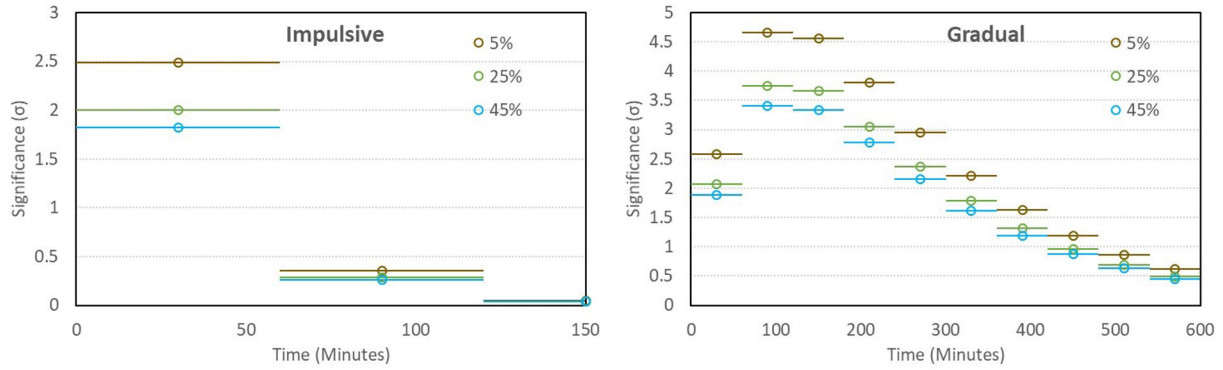

Figure 36. (Example 3) Time profile of statistical significance (per time bin) of a ground level enhancement with 10% peak magnitude relative to GCR, for a single COsmic-ray Soil Moisture Observing System detector with 60-min resolution and volumetric water content from 5% to 45%.

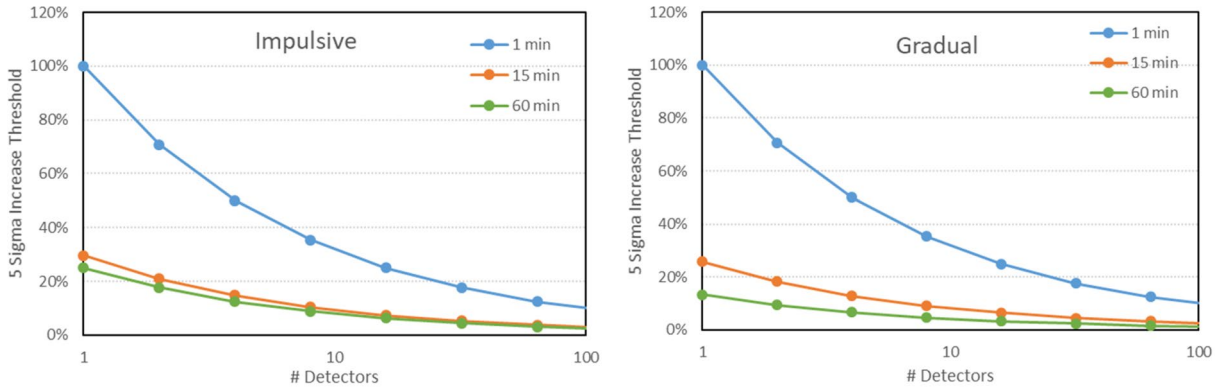

Figure 37. Peak event magnitude 5σ detection threshold as a function of the number of aggregated COsmic-ray Soil Moisture Observing System detectors for impulsive event (LHS) and gradual event (RHS).

the additional counts would all feature in a single counting bin, such a signal could easily be dismissed as erroneous (and we are not accounting for possible detector saturation at such a high neutron flux). This increase is substantially lower than the 900-fold (90%, 000%) increase observed by Martin & Alves, in part due to the very different detector response functions, but also due to the shorter assumed detector-to-source distance of <500 m.

COSMOS detectors have a very different response function, with a falling rather than rising response above 1 MeV. We estimate the net detection efficiency when combined with the Carlson ground level spectrum to be of the order of 1%. For a neutron fluence of 1 n/cm^2, we estimate an additional 12 counts would be recorded during a low-altitude TGF. For a background count rate of ∼1,500 counts per hour for an equatorial detector this corresponds to a ∼50% increase in count rate in 1-min bins, not dissimilar to the GLNM prediction. The similarity occurs because both detector types have relatively poor counting efficiency at ∼MeV energies compared to other parts of the neutron spectrum (lower energies for COSMOS, higher energies for GLNM). At current COSMOS time resolutions of 30 min to 1 h, this would represent an increase of <1%, which would not be visible in the count rate series.

Such modest increases are unlikely to pose a threat to ground level infrastructure. However, the threat to aviation could be more considerable as the distance between target and source could be very short. An attempt to quantify this threat was made by Tavani et al. (2013), by parameterizing various radiation quantities and damage effects (including neutron fluence and SEE rate) in terms of particle production number and cylindrical beam radius. As these parameters each have potential ranges extending over orders of

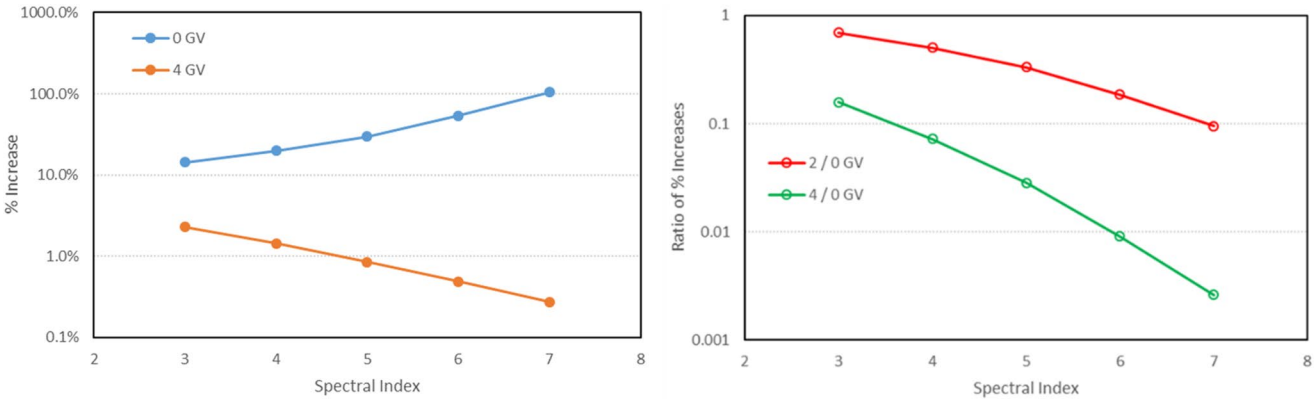

Figure 38. (LHS) Expected % increase in COsmic-ray Soil Moisture Observing System detector count rate as a function of spectral index for an event causing a 10% increase at 2 GV. Blue and orange curves show increases at 0 and 4 GV respectively. (RHS) Hypothetical ratios of count rate increase for separate detectors at two rigidities. The red line shows the ratio for one detector at 2 GV and the other at 0 GV; the green line shows the ratio for one detector at 4 GV and the other at 0 GV.

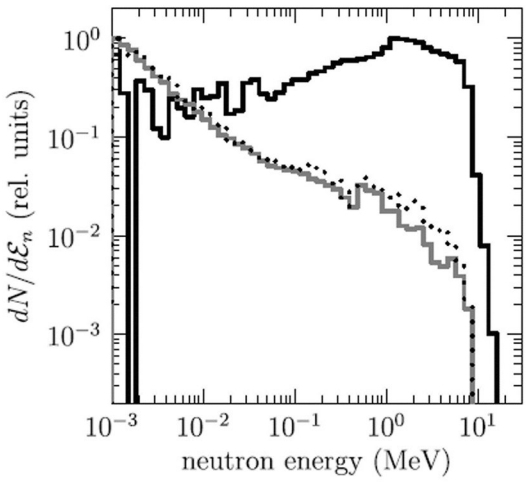

Figure 39. Simulated spectra for terrestrial gamma ray flash source neutrons (black line), upper atmosphere escape neutrons (gray line) and ground level neutrons (dots) in relative units (reproduced from Carlson et al., 2010).

magnitude, this leads to an extremely wide range for the neutron fluence induced by a TGF. Neutron production in their analysis is due to interactions between gamma rays and an aircraft hull, rather than with atmospheric molecules.

Using a standard SEU upset cross section, the authors claim a critical threshold for neutron fluence of 10^6 n/cm^2, with a potential maximum fluence of 10^9 n/cm^2. The neutron spectrum they derive is similar to the source spectrum in Carlson et al. (2010). However, the authors take no account of the how the SEU cross section varies as a function of neutron energy. This is known to rise steeply from 1 to 10 MeV (Dyer et al., 2006), leading to considerable uncertainty in the prediction of SEU from neutrons in this range (Hands et al., 2009; Quinn et al., 2018). The authors also seem to assume that a single SEU in a standard size SRAM represents a significant problem, whereas this is extremely unlikely to be the case. Nonetheless, even though a fluence of 10^6 n/cm^2 (predominantly <10 MeV) may not represent a critical threat to avionics in terms of SEUs, the probability of single event latch-up (SEL), single event burnout (SEB) and other potentially destructive phenomena could be high in this environment (Hands et al., 2011). However, these cross sections are also more significant at neutron energies above 10 MeV, and we estimate that only ~4% of neutrons in the Tavani spectrum are this energetic. The large uncertainty in the fluence of fast neutrons is problematic in terms of using this parametrized model to gauge risk to avionics. However, even at the lower end of fluence for the parameter range specified (10^3 n/cm^2) the average neutron flux over a 1 s timescale is orders of magnitude greater than both the background level at altitude, and the ground level environment predicted for TGFs elsewhere. There is clearly potential for SEEs to occur in any susceptible microelectronic component that finds itself in close proximity to a TGF, but there remains a large degree of uncertainty in quantifying this threat. An aircraft radiation detector capable of millisecond resolution, would be invaluable in potentially capturing empirical evidence of this phenomenon and gauging the scale of its effect on the local aircraft radiation environment.

5. Scope for Enhancing the Existing Network

5.1. Time Resolution and Data Transmission

At present, the COSMOS-UK network is configured to log neutron counts from the CRS2000/B every 30 min; this is the highest time resolution of counts recorded. For space weather events, there can be a need to detect events with very fast rise times of seconds, and to report or send alerts for such events as soon as they are detected. This places a requirement on the network to

1. Log neutron counts at much faster rates than the current configuration and
2. Instantaneously send alerts to the relevant space weather data centers when certain events are detected.

In this feasibility study, both aspects were investigated, and tested under laboratory conditions. For this trial, the data logger (model CR3000, Campbell Scientific Ltd., Shepshed, Leicestershire, UK) was programmed to request the accumulated neutron counts every 10 s, from the pulse module within the CRS2000/B. These values of counts per 10 s were logged in a data table (with air pressure, temperature and relative humidity) on the data logger and transmitted to the UKCEH data server. This trial was conducted using a wireless router/modem (cellular gateway), transmitting data over a mobile phone network, necessitating the modem to be always on, ready to transmit data. During the test, all of the other sensors were also interrogated, and data logged normally to ensure that the data logger has sufficient processing time to maintain normal network data acquisition, as well as the additional new load of the 10 s neutron count logging.

There are rare drop-outs, where no data from the pulse module were received by the logger. These missed values (only 0.1% of all counts logged) are so rare that they are unlikely to have any impact on a space weather application. The impact, if any, would be limited to a 10 s delay in detecting an event at a single station

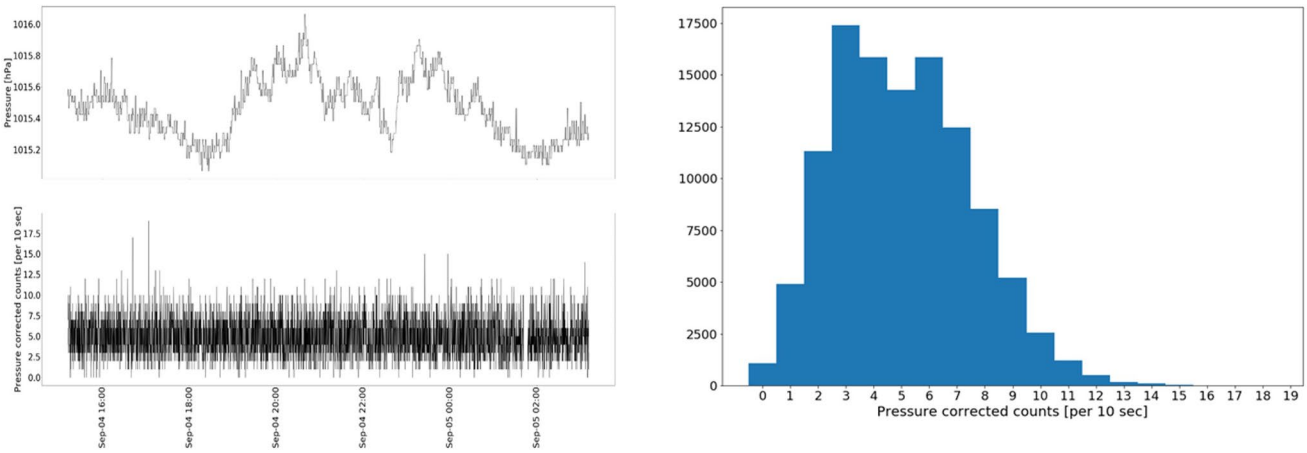

Figure 40. (LHS) Sample of logged 10 s neutron count data. (RHS) histogram of all counts over 2 weeks.

(and the probability that more than one station would be affected in this way, in the same 10 s interval is very low). A sample of the successfully acquired and telemetered data is shown in Figure 40 (LHS). This trial was run over a 2-week period, and a histogram (Figure 40 RHS) shows the distribution all of the pressure-corrected counts for the whole period.

6. Feasibility Assessment

The objective of this study is to evaluate whether the UK COSMOS soil moisture sensor network can be dual-purposed to be an effective alert system for space weather events that pose a hazard to ground level infrastructure and the aviation sector. We have shown through analysis of existing data and simulations of hypothetical events, that COSMOS detectors are sensitive to the changes in the ground level radiation environment that occur during such events, and upgrades to the network that would enable an effective GLE alert system are feasible. A summary of requirements and recommendations to implement such a system are outlined below.

6.1. Count Rate

A typical count rate for a single UK COSMOS detector is of the order of 1,000–2,000 counts per hour depending on local conditions. This is substantially lower than that of a standard design (6-NM64) ground level neutron monitor, which typically records ~70 counts per second (250,000 counts per hour) in a mid-latitude location. This is partly due to the deliberate amplification of neutron flux in the design of neutron monitors, which makes them especially sensitive to high energy neutrons. However, in spite of the substantial differences in response function between these detectors, our analysis shows that the expected percentage increases during a GLE event are similar. This means that, to a first approximation, recreating the count rate of a neutron monitor for both background and GLE conditions (if that were necessary) would simply be a matter of aggregating counts from a larger number of COSMOS detectors. This would imply ~150 sensors, considerably more than the entire UK network of ~50 stations. However, we have shown that sensitivity to even relatively small GLEs can be achieved with a much lower number of sensors (see Figure 37 for example). Indeed, even a single sensor would observe a statistically significant increase in a 1-min averaged count rate for an event of moderate magnitude (>100% increase above background). Nevertheless, to improve the signal-to-noise ratio it would be advantageous to group COSMOS detectors together at selected strategic locations. This would also help to mitigate the impact of a potentially reduced count rate during wet conditions and, in addition, aggregating data from geographically separated stations would compensate for the effect of dynamic local moisture conditions, except during very widespread rainfall events.

The optimum approach is therefore to have the ability to aggregate data both locally and nationally. In order to achieve this, we recommend significantly expanding the number of COSMOS detectors in at least two

strategic UK locations, ideally covering the maximum range in rigidity from northern Scotland to southern England. These detector hubs would act like mini neutron monitors, that is, with total count rates in between a single COSMOS detector and a full neutron monitor. To resolve the peak of an impulsive event that leads to 25% increase in background count rate at 5σ significance with 1-min time resolution, 16 co-located detectors are required. This is 100 times smaller than the Feb-56 GLE (ignoring anisotropy), and thus represents a very low detection threshold. Smaller or softer events may not be observed in a statistically significant way, but such events are very unlikely to pose a threat to critical infrastructure, even at high altitude and latitude.

6.2. Time Resolution

Unlike improvements to count rate, which are useful, improvements to time resolution are essential for the COSMOS network to serve as an effective GLE alert system. The existing half-hourly resolution of the UK network may just be sufficient to monitor the progress of a gradual GLE as it unfolds over many hours, but it is inadequate for an impulsive GLE with a rise-time potentially below 1 min. One minute resolution is both an achievable and a desirable capability for an enhanced COSMOS network. Such an enhancement would make the time resolution comparable to the ground level neutron monitor network that is currently the basis of a number of GLE alert services. Defining the criteria for triggering a GLE alert based on COSMOS data is out of scope for this study and would depend heavily on the number of detectors aggregated in a collective count rate as well as other factors.

The volume of data that would be required to be collected and transmitted for a 1-min resolution service is relatively small and, as we have demonstrated, achievable with only minor modifications to existing network infrastructure. The estimated cost for such an upgrade is £1,000 per station, with additional costs of up to £150,000 for cybersecurity considerations, thus a total cost of the order of £200,000.

Ideally 1-min data would be available in real time for all UK stations. However, in the near term it may be more feasible to roll out the capacity to a smaller number of stations, that is, those selected as strategic hubs for placing multiple detector tubes together to increase overall count rate. Sub-minute time resolution may be achievable in a similar way, though it is questionable whether this would add anything practically to the observation of GLEs. Very fine time resolution would be useful for resolving other phenomena, such as TGFs. However, as these are expected primarily in tropical locations, this is a not a high priority for the UK network.

6.3. Geographical Distribution

The United Kingdom spans a geomagnetic cut-off rigidity range that potentially leads to dramatic differences in the impact of space weather. In quiescent conditions this range is approximately 0.8–3.0 GV (from the Shetlands to Cornwall), but the lower end of this range could drop to zero during the disturbed conditions of a geomagnetic storm. Regardless of the precise range, a ΔR of $\sim$2 GV is very useful for inferring information on the primary proton spectrum of a GLE event, which is important for extrapolating from UK ground level measurements to other altitudes and latitudes. While there are several stations in south west England, the current northernmost UK COSMOS station is at Glensaugh in Aberdeenshire, with a latitude of 56.9° and a corresponding cut-off rigidity (quite-time) of 1.5 GV. Although this is sufficiently different from the lower latitude stations to be useful, maximizing capacity to infer spectral information by establishing COSMOS stations even further north would be sensible.

Examples of count rate ratios during a GLE are plotted in Figure 38. While these are heavily dependent on the spectral index of the GLE proton spectrum, it is clear that as broad a spread in rigidity range as possible would maximize the ratio and improve the fidelity of extracting information on spectral index. This is why we recommend that one of the proposed strategic detector hubs be located in as high a latitude as is practical, whether that be at Glensaugh or elsewhere. If higher latitude locations are not suitable for such a hub, it would still be useful to establish regular COSMOS stations at such locations in order to further exploit the rigidity range of the United Kingdom.

6.4. Adjustment for Local Conditions

The primary function of the COSMOS network will remain hydrological. Secular variations in count rate due to cosmic ray modulation are already accounted for in the derivation of soil moisture from COSMOS count rates. GLEs and Forbush decreases are considered as noise rather than signal in this context. However, rapid changes in local soil moisture conditions could affect the analysis of the same data in a space weather context, for example during gradual GLEs and Forbush decreases. Fortunately, the impact of such local environment effects would be far lower for GLEs of greater magnitude.

The ability to "correct" COSMOS count rates so as to remove the effect of local soil moisture (as well as pressure, humidity etc.) would nevertheless be advantageous. Although implementing such a correction is out of scope for this paper, we recommend that this work is encouraged so that eventually users of the COSMOS network have the option to view the data with this correction applied. This would make interpretation of the data very similar to that of neutron monitors, which is already familiar to many in the space weather community.

6.5. Complementary Data Sources

The UK COSMOS network has been identified as a novel source of space weather data with the potential to be a key national asset for the protection of infrastructure from future GLE events. However, it should not be regarded as a sufficient solution to address space weather impacts in isolation. The existing ground level neutron monitor network, although completely independent of the United Kingdom, currently holds the most important capability to monitor the global impact of GLEs and is likely to continue to do so for the foreseeable future. Wherever possible, the United Kingdom should support the maintenance of the GLNM network, both as a stakeholder in international station data and as a potential location for an addition to the network.

The most valuable source of data for the aviation sector is, of course, *in situ* data from in-flight monitors. The United Kingdom should invest in the development and routine deployment of calibrated monitors on regular high-latitude (most likely North Atlantic) routes to maximize the likelihood of capturing a GLE when one occurs. Ultimately these data should be fed into a real-time alert system that ingests multiple data sources. However, even before such a comprehensive service is developed, these data would be invaluable for retrospective calculation of GLE event characteristics and the dose received by passengers and crew. The viability of bespoke high-altitude measurement platforms for radiation monitoring, such as quick-launch weather balloons and UAVs, should also be fully explored in future UKRI research and development activities. Civilian flight routes from the United Kingdom are particularly vulnerable to space weather impacts, but this situation can be significantly ameliorated through targeted monitoring and warning systems, including both those based *in situ* and on the ground. The UK COSMOS network is well-placed to be an integral part of such future systems.

7. Conclusions

Data from the COSMOS world-wide network of soil moisture monitors over the last 10 years have been examined for signatures of space weather events giving both Forbush decreases and sharp increases from GLEs. While the former are clearly visible (and analysis of them will be reported separately), the two rather small GLEs in this period are only barely discernible. However, simulations of detector response show that significant GLEs, such as have occurred historically, would be readily detected. The UK COSMOS network covers a wide range of geomagnetic latitude and this could be valuably extended by siting monitors in Shetland. Required improvements to time resolution and data transmission could be easily implemented, together with aggregating data from multiple detectors, to provide an effective UK space weather warning system for radiation hazards to aviation and ground level safety critical systems. This would complement other UK programmes to monitor radiation on aircraft and spacecraft. It is recommended that work on dual-purposing COSMOS-UK detectors for the protection of UK critical infrastructure from space weather be initiated as soon as possible in order to detect events in the new solar cycle 25.

Data Availability Statement

The data from the figures in this article are available at https://doi.org/10.5281/zenodo.4757169.

Acknowledgments
This work was funded by the UK Natural Environments Research Council (NERC) under the Digital Environments programme ("MOSAIC" project, grant no. NE/T005734/1). We acknowledge support from industrial partners EDF Energy (UK) and Hydroinnova LLC, and the UK Met Office. We also acknowledge the NMDB database (www.nmdb.eu), founded under the European Union's FP7 programme (contract no. 213007) for providing data, and the PIs of individual neutron monitors at: Kiel (Institut fur Experimentelle und Angewandte Physik, Christian-Albrechts-Universitat zu Kiel, Germany), Oulu (Sodankyla Geophysical Observatory of the University of Oulu, Finland), Inuvik (University of Delaware Department of Physics and Astronomy and the Bartol Research Institute, USA).

References

Asvestari, E., Willamo, T., Gil, A., Usoskin, I., Kovaltsov, G., Mikhailov, V., & Mayorov, A. (2017). Analysis of Ground Level Enhancements (GLE): Extreme solar energetic particle events have hard spectra. *Advances in Space Research*, *60*(4), 781–787. https://doi.org/10.1016/j.asr.2016.08.043

Baatz, R., Bogena, H., Hendricks Franssen, H. J., Huisman, J., Montzka, C., & Vereecken, H. (2015). An empirical vegetation correction for soil water content quantification using cosmic ray probes. *Water Resources Research*, *51*(4), 2030–2046. https://doi.org/10.1002/2014wr016443

Babich, L., Kudryavtsev, A. Y., Kudryavtseva, M., & Kutsyk, I. (2008). Atmospheric gamma-ray and neutron flashes. *Journal of Experimental and Theoretical Physics*, *106*(1), 65–76. https://doi.org/10.1134/s1063776108010056

Belov, A., Eroshenko, E., Mavromichalaki, H., Plainaki, C., & Yanke, V. (2005). Solar cosmic rays during the extremely high ground level enhancement on 23 February 1956. *Annales Geophysicae*, *23*(6), 2281–2291. https://doi.org/10.5194/angeo-23-2281-2005

Cannon, P., Angling, M., Barclay, L., Curry, C., Dyer, C., Edwards, R., et al. (2013). *Extreme space weather: Impacts on engineered systems and infrastructure*. Royal Academy of Engineering.

Carlson, B., Lehtinen, N. G., & Inan, U. S. (2010). Neutron production in terrestrial gamma ray flashes. *Journal of Geophysical Research*, *115*(A4). https://doi.org/10.1029/2009JA014696

Chilingarian, A., Daryan, A., Arakelyan, K., Hovhannisyan, A., Mailyan, B., Melkumyan, L., et al. (2010). Ground-based observations of thunderstorm-correlated fluxes of high-energy electrons, gamma rays, and neutrons. *Physical Review D*, *82*(4), 043009. https://doi.org/10.1103/physrevd.82.043009

Clem, J. M., & Dorman, L. I. (2000). Neutron monitor response functions. In *Cosmic rays and Earth* (pp. 335–359). Springer. https://doi.org/10.1007/978-94-017-1187-6_16

Cooper, H. M., Bennett, E., Blake, J., Blyth, E., Boorman, D., Cooper, E., et al. (2021). COSMOS-UK: National soil moisture and hydrometeorology data for environmental science research. *Earth System Science Data*, *13*(4), 1737–1757. https://doi.org/10.5194/essd-13-1737-2021

Copeland, K., & Atwell, W. (2019). Flight safety implications of the extreme solar proton event of 23 February 1956. *Advances in Space Research*, *63*(1), 665–671. https://doi.org/10.1016/j.asr.2018.11.005

Dwyer, J., Smith, D., & Cummer, S. (2012). High-energy atmospheric physics: Terrestrial gamma-ray flashes and related phenomena. *Space Science Reviews*, *173*(1–4), 133–196. https://doi.org/10.1007/s11214-012-9894-0

Dwyer, J., Smith, D., Uman, M., Saleh, Z., Grefenstette, B., Hazelton, B., & Rassoul, H. (2010). Estimation of the fluence of high-energy electron bursts produced by thunderclouds and the resulting radiation doses received in aircraft. *Journal of Geophysical Research*, *115*(D9). https://doi.org/10.1029/2009JD012039

Dyer, C., Hands, A., Ford, K., Frydland, A., & Truscott, P. (2006). Neutron-induced single event effects testing across a wide range of energies and facilities and implications for standards. *IEEE Transactions on Nuclear Science*, *53*(6), 3596–3601. https://doi.org/10.1109/tns.2006.886207

Dyer, C., Hands, A., Ryden, K., & Lei, F. (2018). Extreme atmospheric radiation environments and single event effects. *IEEE Transactions on Nuclear Science*, *65*(1), 432–438. https://doi.org/10.1109/TNS.2017.2761258

Dyer, C., Lei, F., Hands, A., & Truscott, P. (2007). Solar particle events in the QinetiQ atmospheric radiation model. *IEEE Transactions on Nuclear Science*, *54*(4), 1071–1075. https://doi.org/10.1109/tns.2007.893537

Evans, J. G., Ward, H. C., Blake, J. R., Hewitt, E. J., Morrison, R., Fry, M., et al. (2016). Soil water content in southern England derived from a cosmic-ray soil moisture observing system—COSMOS-UK. *Hydrological Processes*, *30*(26), 4987–4999. https://doi.org/10.1002/hyp.10929

Hands, A., Dyer, C. S., & Lei, F. (2009). SEU rates in atmospheric environments: Variations due to cross-section fits and environment models. *IEEE Transactions on Nuclear Science*, *56*(4), 2026–2034. https://doi.org/10.1109/TNS.2009.2013466

Hands, A., Lei, F., Ryden, K., Dyer, C., Underwood, C., & Mertens, C. (2017). New data and modeling for single event effects in the stratospheric radiation environment. *IEEE Transactions on Nuclear Science*, *64*(1), 587–595. https://doi.org/10.1109/TNS.2016.2612000

Hands, A., Morris, P., Ryden, K., Dyer, C., Truscott, P., Chugg, A., & Parker, S. (2011). Single event effects in power MOSFETs due to atmospheric and thermal neutrons. *IEEE Transactions on Nuclear Science*, *58*(6), 2687–2694. https://doi.org/10.1109/TNS.2011.2168540

International Electro-technical Commission (2017). *Process management for avionics—Atmospheric radiation effects—Part 6: Extreme Space Weather*. Retrieved from https://webstore.iec.ch/publication/59928

Jiggens, P., Clavie, C., Evans, H., O'Brien, T., Witasse, O., Mishev, A., et al. (2019). In situ data and effect correlation during September 2017 solar particle event. *Space Weather*, *17*(1), 99–117. https://doi.org/10.1029/2018SW001936

Köhli, M., Schrön, M., & Schmidt, U. (2018). Response functions for detectors in cosmic ray neutron sensing. *Nuclear Instruments and Methods in Physics Research Section A: Accelerators, Spectrometers, Detectors and Associated Equipment*, *902*, 184–189. https://doi.org/10.1016/j.nima.2018.06.052

Köhli, M., Schrön, M., Zreda, M., Schmidt, U., Dietrich, P., & Zacharias, S. (2015). Footprint characteristics revised for field-scale soil moisture monitoring with cosmic-ray neutrons. *Water Resources Research*, *51*(7), 5772–5790. https://doi.org/10.1002/2015wr017169

Lockwood, J. (1971). Forbush decreases in the cosmic radiation. *Space Science Reviews*, *12*(5), 658–715. https://doi.org/10.1007/BF00173346

Lockwood, J., Webber, W., & Debrunner, H. (1991). The rigidity dependence of Forbush decreases observed at the Earth. *Journal of Geophysical Research*, *96*(A4), 5447–5455. https://doi.org/10.1029/91JA00089

Martin, I. M., & Alves, M. A. (2010). Observation of a possible neutron burst associated with a lightning discharge? *Journal of Geophysical Research*, *115*(A2). https://doi.org/10.1029/2009JA014498

McCracken, K., Moraal, H., & Shea, M. (2012). The high-energy impulsive ground-level enhancement. *The Astrophysical Journal*, *761*(2), 101. https://doi.org/10.1088/0004-637x/761/2/101

McCracken, K., Moraal, H., & Stoker, P. (2008). Investigation of the multiple-component structure of the 20 January 2005 cosmic ray ground level enhancement. *Journal of Geophysical Research*, *113*(A12). https://doi.org/10.1029/2007JA012829

McCracken, K., Shea, M., & Smart, D. (2016). *The short-lived (<2 minutes) acceleration of protons to >13 GeV in association with solar flares*. EGUGA. EPSC2016-9634.

Meier, M. M., Copeland, K., Klöble, K. E., Matthiä, D., Plettenberg, M. C., Schennetten, K., et al. (2020). Radiation in the atmosphere—A hazard to aviation safety? *Atmosphere*, *11*(12), 1358. https://doi.org/10.3390/atmos11121358

Miroshnichenko, L. I. (2018). Retrospective analysis of GLEs and estimates of radiation risks. *Journal of Space Weather and Space Climate*, *8*, A52. https://doi.org/10.1051/swsc/2018042

Mishev, A., Kocharov, L., & Usoskin, I. (2014). Analysis of the ground level enhancement on 17 May 2012 using data from the global neutron monitor network. *Journal of Geophysical Research: Space Physics*, *119*(2), 670–679. https://doi.org/10.1002/2013JA019253

Mishev, A., & Usoskin, I. (2018). Assessment of the radiation environment at commercial jet-flight altitudes during GLE 72 on 10 September 2017 using neutron monitor data. *Space Weather*, *16*(12), 1921–1929. https://doi.org/10.1029/2018SW001946

Mishev, A., & Usoskin, I. (2020). Current status and possible extension of the global neutron monitor network. *Journal of Space Weather and Space Climate*, *10*, 17. https://doi.org/10.1051/swsc/2020020

National Risk Register of Civil Emergencies (2020). Retrieved from https://www.gov.uk/government/publications/national-risk-register-2020

Power, D., Rico-Ramirez, M. A., Desilets, S., Desilets, D., & Rosolem, R. (2021). Cosmic-Ray neutron Sensor PYthon tool (crspy): An open-source tool for the processing of cosmic-ray neutron and soil moisture data. *Geoscientific Model Development Discussions*, *2021*, 1–34. https://doi.org/10.5194/gmd-2021-77

Quinn, H., Watkins, A., Dominik, L., & Slayman, C. (2018). The effect of 1–10-MeV neutrons on the JESD89 test standard. *IEEE Transactions on Nuclear Science*, *66*(1), 140–147.

Rosolem, R., Shuttleworth, W. J., Zreda, M., Franz, T., Zeng, X., & Kurc, S. (2013). The effect of atmospheric water vapor on neutron count in the cosmic-ray soil moisture observing system. *Journal of Hydrometeorology*, *14*(5), 1659–1671. https://doi.org/10.1175/jhm-d-12-0120.1

Schrön, M. (2017). *Cosmic-ray neutron sensing and its applications to soil and land surface hydrology*. Verlag Dr. Hut.

Schrön, M., Köhli, M., Scheiffele, L., Iwema, J., Bogena, H. R., Lv, L., et al. (2017). Improving calibration and validation of cosmic-ray neutron sensors in the light of spatial sensitivity. *Hydrology and Earth System Sciences*, *21*(10), 5009–5030. https://doi.org/10.5194/hess-21-5009-2017

Shea, M., & Smart, D. (1990). A summary of major solar proton events. *Solar Physics*, *127*(2), 297–320. https://doi.org/10.1007/bf00152170

Tavani, M., Argan, A., Paccagnella, A., Pesoli, A., Palma, F., Gerardin, S., et al. (2013). Possible effects on avionics induced by terrestrial gamma-ray flashes. *Natural Hazards and Earth System Sciences*, *13*(4), 1127–1133. https://doi.org/10.5194/nhess-13-1127-2013

Tylka, A. J. (2008). Proton spectra in Ground-Level Enhanced (GLE) solar particle events. *Cosp*, *37*, 3246.

Wada, Y., Enoto, T., Nakamura, Y., Furuta, Y., Yuasa, T., Nakazawa, K., et al. (2019). Gamma-ray glow preceding downward terrestrial gamma-ray flash. *Communications on Physics*, *2*(1), 1–9. https://doi.org/10.1038/s42005-019-0168-y

Winckler, J. R. (1956). Cosmic-ray increase at high altitude on February 23, 1956. *Physical Review*, *104*(1), 220. https://doi.org/10.1103/physrev.104.220

Zreda, M., Shuttleworth, W. J., Zeng, X., Zweck, C., Desilets, D., Franz, T., & Rosolem, R. (2012). COSMOS: The cosmic-ray soil moisture observing system. *Hydrology and Earth System Sciences*, *16*(11), 4079–4099. https://doi.org/10.5194/hess-16-4079-2012